Categorical Refraction at Axion–Duality Junctions

Intersection CFTs and Non-Invertible Symmetry Transmutation in Four-Dimensional Gauge Theory

Rihaan Shah

July 2026

Abstract

We develop a field-theoretic framework for the codimension-two junction formed by the intersection of an axion domain wall and an electromagnetic-duality wall in four-dimensional abelian gauge theory. The basic input is axion electrodynamics on an oriented four-manifold together with a jump $\Delta\theta = 2\pi k$ across a wall W_θ and a duality interface W_g labeled by $g = \left(\begin{smallmatrix} a & b \\ c & d \end{smallmatrix}\right) \in \mathrm{SL}(2,\mathbb{Z})$. The two wall operations fail to commute by the charge-lattice monodromy

$$\mathcal{M}_{k,g} = T_k g T_{-k} g^{-1} = \begin{pmatrix} 1 + kc(a+kc) & k(1-a^2-akc) \\ kc^2 & 1-akc \end{pmatrix},$$

where T_k is the Witten-effect transformation $(q_e, q_m) \mapsto (q_e + kq_m, q_m)$. We prove that, in the uncondensed spin U(1) theory, a trivial topological intersection exists only when $k = 0$ or $c = 0$. Physically, a line operator sent through the junction can come out as several allowed dyonic outcomes, with the junction carrying the charge mismatch that ordinary duality cannot assign to one outgoing line. More generally, for a finite unbroken charge quotient $\Gamma_{\mathrm{em}}/\Lambda_\Sigma$, the compatibility condition is $(\mathcal{M}_{k,g} - \mathrm{id})\Gamma_{\mathrm{em}} \subset \Lambda_\Sigma$. When this condition fails, the intersection must carry nontrivial two-dimensional degrees of freedom: a topological sector, a chiral anomalous theory, or a conformal defect theory. We call the resulting transformation of Wilson, 't Hooft, and dyonic lines categorical refraction:

$$\mathfrak{R}_{k,g}(L_\gamma) = \bigoplus_{\gamma'} V_\gamma^{\gamma'} \otimes L_{\gamma'}.$$

Here $V_\gamma^{\gamma'}$ records the junction states that make each outgoing sector possible. We derive the anomaly inflow constraints, construct candidate compact-boson and finite TQFT junction models, solve a controlled twisted-mode problem near the codimension-two defect, and formulate defect bootstrap equations with categorical recoupling data. Sixteen reproducible Matplotlib figures and accompanying symbolic and numerical scripts are included with the source.

Contents

1 Introduction

Duality walls and axion walls are standard objects in four-dimensional gauge theory, but their intersections are not merely decorative features of a defect network. An axion wall shifts the electric charge of a magnetic object through the Witten effect [1, 2]. An electromagnetic-duality wall acts on the electric-magnetic charge lattice by an element of $\mathrm{SL}(2,\mathbb{Z})$. These operations generally do not commute. When the two walls meet on a two-dimensional surface Σ_2, a Wilson-'t Hooft line transported around the junction returns with a different charge. The junction must therefore carry the missing data.

The purpose of this paper is to give that statement a precise field-theoretic form. We work with a four-dimensional abelian gauge theory with compact gauge group, charge lattice, and quantized theta periodicity. Let

$$S_{\mathrm{bulk}} = \int_{M_4} \left[-\frac{1}{2e^2} F \wedge \star F + \frac{\theta(x)}{8\pi^2} F \wedge F + \frac{f_a^2}{2} \mathrm{d}\theta \wedge \star \mathrm{d}\theta \right],$$

where A is a $\mathrm{U}(1)$ connection, $F = \mathrm{d}A$, and $\theta \sim \theta + 2\pi$ is a periodic axion. Across the wall W_θ the axion jumps by $\Delta\theta = 2\pi k$ in the integral case. A second wall W_g implements a duality transformation

$$g = \begin{pmatrix} a & b \\ c & d \end{pmatrix} \in \mathrm{SL}(2,\mathbb{Z}).$$

The intersection $\Sigma_2 = W_\theta \cap W_g$ is codimension two in M_4. In Lorentzian signature it is a $1+1$ dimensional world sheet; in Euclidean signature it is a conformal defect candidate.

The central claim is not that axion walls, duality walls, non-invertible defects, or defect CFTs are individually new. They are not. The claim is that the intersection of an axion wall with an electromagnetic-duality wall has an intrinsic consistency problem, measured by a charge-lattice commutator, and that the local resolution of this problem defines a constrained two-dimensional quantum field theory. The transformation of extended operators at this two-dimensional locus is generally not an invertible map on single charge sectors. It is a functorial or categorical operation that can split a line into multiple outgoing sectors, attach a surface defect, terminate a line on a junction excitation, or produce an anomalous phase. We call this phenomenon categorical refraction.

The paper has four concrete outputs.

1. A compatibility theorem for topological axion-duality intersections in the uncondensed theory and in quotient charge lattices.

2. An anomaly-inflow framework that identifies what a junction theory must cancel.

3. A categorical refraction law for Wilson-'t Hooft operators, including selection rules and possible multiplicity spaces.

4. A reproducible symbolic and numerical program: monodromy scans, a twisted mode model, a finite conformal-block residual analysis, and sixteen publication-style Matplotlib figures.

The results should be read as a controlled framework rather than a claim that every dynamical model has been solved. We distinguish theorems about charge lattices and anomalies from conjectures about infrared conformality and bootstrap islands. In particular, the numerical bootstrap section is a finite truncation designed to illustrate the constraints and data structures that a full semidefinite bootstrap would use.

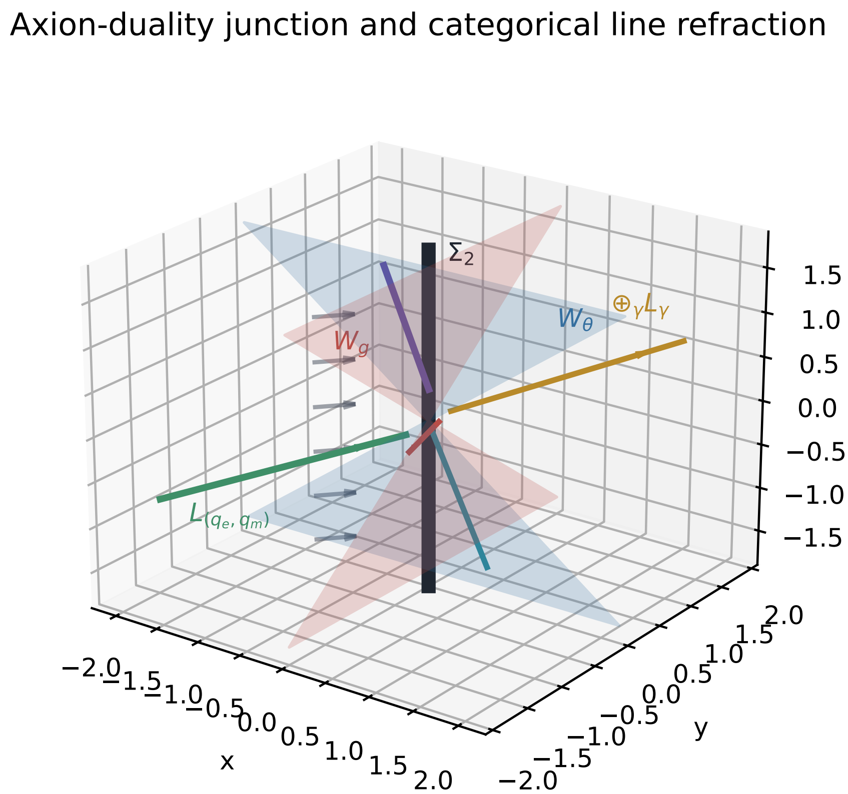

Figure 1: Visual abstract. A spacetime-inspired rendering of an axion wall W_θ, an electromagnetic-duality wall W_g, and their codimension-two intersection Σ_2. Incoming Wilson-'t Hooft lines can refract into several outgoing dyonic sectors. Grey arrows indicate anomaly inflow from the surrounding wall network toward the junction. The figure is schematic but the labels correspond to the charge-lattice construction used in the text.

2 Existing Literature and Novelty Audit

This work sits at the intersection of several mature literatures. The Witten effect and axion electrodynamics explain how theta-angle variation changes electric charge assignments for magnetic objects [1, 2]. Generalized global symmetries provide the language for electric and magnetic one-form symmetries and their defects [4]. Duality walls and boundary duality operations are closely related to the $\mathrm{SL}(2,\mathbb{Z})$ action on three-dimensional theories with abelian symmetry [5] and to boundary conditions in supersymmetric gauge theories [6]. Maxwell theory also has subtle gravitational and duality anomalies [7].

Recent work on non-invertible symmetries in four dimensions is essential background. Half-space gauging constructions produce non-invertible duality defects in 3+1 dimensions [8, 9]. Higher gauging and condensation defects explain why fusion coefficients may themselves be lower-dimensional TQFTs rather than numbers [10]. Higher-categorical formulations and SymTFT methods organize such defects and charges [11, 12, 15]. In axion-Maxwell theory, non-invertible Gauss laws and non-invertible one-form structures have been constructed and related to monopoles, axion strings, and selection rules [13, 14]. Maxwell duality defects on non-spin manifolds and symmetry fractionalization have also been analyzed in detail [16]. Very recent work extends non-invertible duality ideas for Maxwell and Gaillard-Zumino type theories [17, 18].

Defect conformal field theory and the defect bootstrap give the language for local operators supported on the intersection. The formalism of bulk-to-defect OPEs, displacement operators, and codimension-two conformal blocks was developed in [19], with boundary and interface bootstrap methods in [20, 21]. The endpoint bootstrap for conformal line defects [22] is especially suggestive for codimension-changing junctions, although the present setting concerns a two-dimensional intersection in a four-dimensional bulk.

The novelty pursued here is narrower than any claim of inventing these tools. We ask what happens when an axion wall and an electromagnetic-duality wall intersect, and we make the charge-lattice incompatibility the organizing principle. The table below summarizes the distinction.

Reference	Defect setting	What is controlled	Distinction from this work
Witten [1]; Wilczek [2]	theta angle and axion response in 4d gauge theory	Witten effect for monopoles and dyons, axion electrodynamic response	Supplies the axion-wall mechanism but does not include electromagnetic-duality wall intersections.
Gaiotto et al. [4]	higher-form symmetry defects	electric and magnetic one-form symmetries, charged operators, anomaly language	Provides the symmetry framework rather than a specific axion-duality junction theory.
Witten [5]	S, T operations for 3d theories with abelian symmetry	Chern-Simons contact terms and duality operations	Closely related wall technology, but no codimension-two axion-duality intersection.
Hsieh, Tachikawa, Yonekura [7]	Maxwell duality backgrounds	gravitational anomaly of electromagnetic duality	Supplies anomaly constraints for duality, not the junction refraction law.
Choi et al. [8]; Kaidi et al. [9]	non-invertible duality defects in 4d	half-space gauging, duality-defect fusion, one-form SPT data	Treats duality defects themselves; the present work intersects them with axion walls.
Yokokura [13]; Choi, Lam, Shao [14]	axion-Maxwell non-invertible symmetries	axion selection rules, monopoles, strings, non-invertible Gauss laws	Gives essential axion input, but not the $\mathrm{SL}(2,\mathbb{Z})$ wall-junction CFT.

Table 1: Novelty audit, field-theory inputs. These works establish the ingredients used here: axion response, higher-form symmetry, electromagnetic duality, and non-invertible defects.

Reference	Defect setting	What is controlled	Distinction from this work
Roumpedakis et al. [10]	higher gauging and condensation defects	TQFT-valued fusion coefficients and non-invertible condensation	Explains why refraction coefficients may be spaces or sectors rather than numbers.
Bhardwaj et al. [11]; Bhardwaj, Schafer-Nameki [15]	higher-categorical and SymTFT symmetries	categorical charges, higher morphisms, one-higher-dimensional organization	Provides the organizational language, while this paper computes a concrete charge-lattice obstruction.
Kan, Kawabata, Wada [16]; Meynet et al. [17]	Maxwell duality and fractionalization	duality defects, global-form subtleties, enhanced duality symmetry	Closest Maxwell-duality context, but without the axion-wall commutator theorem.
Billo et al. [19]; Liendo et al. [20]; Gliozzi et al. [21]	defect CFT and bootstrap	bulk-to-defect OPEs, displacement data, boundary/interface crossing	Supplies CFT kinematics used for the junction spectrum and bootstrap equations.
Lanzetta et al. [22]	endpoint bootstrap for line defects	endpoint spectra and crossing constraints	Motivates junction bootstrap methods, but the present defect is a 2d axion-duality intersection in 4d.
Present work	$W_\theta \cap W_g$ in 4d axion electrodynamics	monodromy theorem, anomaly inflow, categorical refraction, candidate junction CFT data	Treats intersecting axion and electromagnetic-duality walls as the central object.

Table 2: Novelty audit, categorical and bootstrap inputs. The present work uses these tools to formulate the axion-duality intersection and its line-operator refraction law.

3 Axion Electrodynamics and Electromagnetic Duality

We fix conventions carefully because the junction theorem depends on the global charge lattice. Let M_4 be oriented. A compact U(1) gauge field is a connection on a line bundle with

$$\frac{1}{2\pi}\int_C F \in \mathbb{Z}$$

for closed two-cycles C. The electric-magnetic charge lattice for Wilson-'t Hooft lines is

$$\Gamma_{\text{em}} = \mathbb{Z}e \oplus \mathbb{Z}m, \qquad \gamma = \begin{pmatrix} q_e \\ q_m \end{pmatrix}.$$

The Dirac pairing is

$$\langle \gamma, \gamma' \rangle = q_e q_m' - q_m q_e' = \gamma^T \Omega \gamma', \qquad \Omega = \begin{pmatrix} 0 & 1 \\ -1 & 0 \end{pmatrix}.$$

A choice of global form, spin structure, and line statistics can refine this lattice. For the main theorem we first use the spin U(1) theory with the full unimodular lattice $\mathbb{Z}^2$. Later we pass to quotients and condensed sublattices.

With constant coupling, introduce

$$\tau = \frac{\theta}{2\pi} + \frac{4\pi i}{e^2}.$$

The Maxwell equations and Bianchi identity can be written in terms of the pair (F, G), where

$$G = -2\pi \frac{\delta S}{\delta F} = \frac{2\pi}{e^2} \star F - \frac{\theta}{2\pi} F$$

up to the Lorentzian sign convention. The pair transforms as an $\mathrm{SL}(2,\mathbb{Z})$ doublet under electromagnetic duality. On charges,

$$\gamma \mapsto g\gamma, \qquad g = \begin{pmatrix} a & b \\ c & d \end{pmatrix} \in \mathrm{SL}(2,\mathbb{Z}).$$

The standard generators are

$$S = \begin{pmatrix} 0 & -1 \\ 1 & 0 \end{pmatrix}, \qquad T = \begin{pmatrix} 1 & 1 \\ 0 & 1 \end{pmatrix}.$$

The T operation shifts $\theta \mapsto \theta + 2\pi$ and acts on line charges as

$$T : \begin{pmatrix} q_e \\ q_m \end{pmatrix} \mapsto \begin{pmatrix} q_e + q_m \\ q_m \end{pmatrix}.$$

An axion wall of jump $\Delta\theta = 2\pi k$ therefore acts by

$$T_k = \begin{pmatrix} 1 & k \\ 0 & 1 \end{pmatrix}.$$

The sign is fixed by taking the electric charge of a monopole to change by kq_m when it crosses the wall in the positive normal direction. Reversing the orientation of the wall sends $k \mapsto -k$.

For $\Delta\theta$ not an integral multiple of 2π, the wall response is not a standalone compact U(1) Chern-Simons theory with the same charge lattice. A fractional jump can be meaningful in the presence of additional topological order, a restricted charge spectrum, a background rather than dynamical gauge field, or spin$_c$ refinements. Unless stated otherwise, the phrase "axion wall of level k" means $\Delta\theta = 2\pi k$ with $k \in \mathbb{Z}$.

4 Higher-Form and Non-Invertible Symmetries

In pure Maxwell theory without dynamical electric or magnetic matter, there are electric and magnetic one-form symmetries. Their schematic currents are

$$J_e^{(2)} = \frac{1}{2\pi} G, \qquad J_m^{(2)} = \frac{1}{2\pi} F.$$

Wilson lines are charged under the electric one-form symmetry and 't Hooft lines are charged under the magnetic one-form symmetry. Dynamical electric charges explicitly break the electric one-form symmetry; dynamical monopoles break the magnetic one-form symmetry. In a compact theory with complete charge spectrum, only suitable finite subgroups may remain as exact symmetries.

The axion coupling changes the conservation and gauge-invariance properties of electric flux. The Witten effect implies that a monopole transported through axion field space can acquire electric charge. In modern language, the naive electric one-form symmetry mixes with axion shifts, Page charge, and possible non-invertible defects [13, 14]. In the present paper we do not need the most general axion symmetry category. We use three facts:

1. the exact charge lattice has a symplectic Dirac pairing;
2. an integral axion jump acts by T_k on this lattice;
3. a non-invertible wall may have fusion coefficients valued in topological sectors or vector spaces rather than integers.

Let $\mathcal{D}_g$ denote a duality defect. If g is an honest invertible duality of the full theory at the given coupling, then $\mathcal{D}_g$ is invertible. If g is implemented by gauging in a half-space, by summing over a sublattice, or by extending the theory with an auxiliary topological sector, then the defect can be non-invertible. A typical fusion rule has the form

$$\mathcal{D}_g \otimes \mathcal{D}_g^\dagger = \bigoplus_\alpha \mathcal{U}_\alpha,$$

where the $\mathcal{U}_\alpha$ are invertible higher-form symmetry defects or lower-dimensional TQFT sectors. This is the structural origin of the direct sum in categorical refraction.

5 Axion and Duality Walls

An axion wall is a codimension-one locus where θ changes. If the wall is sharp and oriented, the topological part of the bulk action gives

$$\frac{1}{8\pi^2} \int_{M_4} \theta F \wedge F = \frac{1}{8\pi^2} \int_{M_4} \mathrm{d}\theta \wedge A \wedge \mathrm{d}A \quad \text{locally},$$

so a jump $\Delta\theta = 2\pi k$ induces a wall response

$$S_{W_\theta}^{\mathrm{loc}} = \frac{k}{4\pi} \int_{W_\theta} A \wedge \mathrm{d}A.$$

This formula is local. Globally it must be interpreted by differential cohomology or by extending to a four-manifold bounding the wall. On a spin three-manifold, integer k gives a well-defined spin Chern-Simons level in the standard normalization. On a non-spin three-manifold with a purely bosonic U(1) gauge field, the allowed levels are more constrained unless the gauge field is spin$_c$ or line statistics are adjusted. These familiar qualifications are not optional: they decide whether a proposed wall can exist without extra topological order.

A duality wall relates gauge fields on its two sides. For the S wall one may write a local topological coupling

$$S_S = \frac{1}{2\pi} \int_{W_g} A_L \wedge \mathrm{d}A_R,$$

with sign and orientation chosen so that variations impose the duality-twisted matching of electric and magnetic fields. General $g \in \mathrm{SL}(2, \mathbb{Z})$ walls can be built from S and T generators, or represented by abelian Chern-Simons data on the wall whenever a local Lagrangian description exists. In a non-invertible construction, this wall includes a sum over auxiliary gauge fields or a gauging operation on one side of spacetime.

The intersection Σ_2 is the place where the two wall descriptions must be compatible. If one approaches a point near Σ_2 from four quadrants in the transverse plane, the coupling and charge frame change by T_k across W_θ and by g across W_g. The loop around Σ_2 therefore acts by

$$\mathcal{M}_{k,g} = T_k g T_{-k} g^{-1}$$

on electric-magnetic charges. A nontrivial $\mathcal{M}_{k,g}$ is a monodromy defect localized at Σ_2.

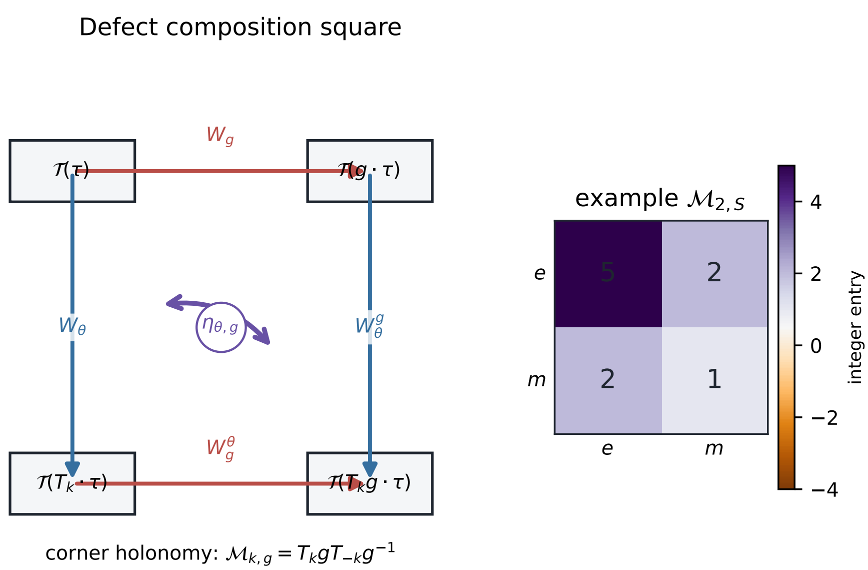

Figure 2: Defect composition square. The two paths around the square correspond to composing the axion wall and the duality wall in different orders. The two-dimensional junction is a 2-morphism $\eta_{\theta,g}$ between the two compositions. The monodromy $\mathcal{M}_{k,g}$ measures the failure of strict commutativity.

6 Intersections of Codimension-One Defects

We now formulate the consistency problem in a way independent of microscopic wall Lagrangians. Let a small circle $S^1_\perp$ link Σ_2 in the transverse plane. A line operator ending outside the circle can be transported around $S^1_\perp$. If the defect network is topological and the junction is trivial, the charge label must return to itself. If it does not, either the line has changed by an operator living on Σ_2 or the proposed trivial junction is inconsistent.

Let $\Lambda_\Sigma \subset \Gamma_{\rm em}$ be the sublattice of electric-magnetic charges that can be absorbed at the junction. It may be zero for a completely uncondensed junction, $N\Gamma_{\rm em}$ for a finite quotient, or a Lagrangian sublattice for a gapped boundary of an auxiliary TQFT. The necessary charge condition is

$$(\mathcal{M}_{k,g} - \mathrm{id})\Gamma_{\rm em} \subset \Lambda_\Sigma.$$

This condition has two meanings. First, a charge transported around the junction can differ from the original charge only by a charge that can end on Σ_2. Second, the unbroken one-form charge group $\Gamma_{\rm em}/\Lambda_\Sigma$ sees no monodromy. It is therefore the natural general compatibility condition.

Definition 6.1 (Topologically trivial junction)**.** *In a fixed charge lattice $\Gamma_{\rm em}$, a junction is topologically trivial relative to a condensed sublattice Λ_Σ if it has no intrinsic junction superselection sectors and all line monodromies act trivially on $\Gamma_{\rm em}/\Lambda_\Sigma$.*

Theorem 6.2 (Junction consistency theorem)**.** *Let $\Gamma_{\rm em} = \mathbb{Z}^2$ with the standard Dirac pairing, and let the axion wall have level $k \in \mathbb{Z}$. Let W_g be labeled by*

$$g = \begin{pmatrix} a & b \\ c & d \end{pmatrix} \in \mathrm{SL}(2, \mathbb{Z}).$$

For a topologically trivial uncondensed junction, so that $\Lambda_\Sigma = 0$, the necessary and sufficient charge-lattice compatibility condition is

$$T_k g T_{-k} g^{-1} = \mathrm{id}.$$

For $k \neq 0$, this holds if and only if $c = 0$. Equivalently, a nonzero integral axion wall commutes only with duality transformations that preserve the magnetic sublattice.

Proof. Direct multiplication gives

$$T_k g T_{-k} g^{-1} = \begin{pmatrix} 1 + kc(a + kc) & k(1 - a^2 - akc) \\ kc^2 & 1 - akc \end{pmatrix}.$$

If this matrix is the identity and $k \neq 0$, the lower-left entry gives $kc^2 = 0$, hence $c = 0$. Conversely, if $c = 0$, the condition $ad - bc = 1$ gives $ad = 1$, so $a = d = \pm 1$. Then the upper-right entry is $k(1 - a^2) = 0$, and the remaining entries are those of the identity. This proves the statement. The condition is also sufficient at the level of charge monodromy because all charge labels return to themselves. □

The physical content of the condition $c = 0$ is simple. The Witten effect only acts on objects with magnetic charge: crossing the axion wall changes q_e by kq_m. A duality transformation with $c \neq 0$ converts part of an electric line into magnetic charge before or after the axion jump. The axion wall then sees different magnetic charge in the two orders of crossing, so the induced electric shift is different. If $c = 0$, magnetic charge is preserved by the duality wall, and the axion-induced electric shift is the same in both orders. This is why upper triangular dualities avoid the hyperbolic obstruction while genuine electric-magnetic rotations such as S do not.

Corollary 6.3 (Hyperbolic obstruction)**.** *For $kc \neq 0$, the monodromy has*

$$\mathrm{Tr}\mathcal{M}_{k,g} = 2 + k^2 c^2 > 2.$$

Thus every nontrivial axion-duality commutator in the full integral lattice is hyperbolic. It cannot be removed by a finite order relabeling of charges.

Theorem 6.4 (Quotient compatibility)**.** *Let Λ_Σ be a sublattice of Γ_{em} describing charges that may be absorbed at the junction. A topologically trivial junction relative to the quotient $\Gamma_{\text{em}}/\Lambda_\Sigma$ requires and, at the level of charge monodromy, is equivalent to*

$$(\mathcal{M}_{k,g} - \text{id})\Gamma_{\text{em}} \subset \Lambda_\Sigma.$$

For $\Lambda_\Sigma = N\Gamma_{\text{em}}$, this is the congruence condition

$$\mathcal{M}_{k,g} \equiv I \pmod{N}.$$

Proof. Transport of a line of charge γ around the junction changes its label to $\mathcal{M}_{k,g}\gamma$. In the quotient theory, the two labels are the same precisely when $\mathcal{M}_{k,g}\gamma - \gamma \in \Lambda_\Sigma$. Requiring this for all γ gives the displayed inclusion. For $\Lambda_\Sigma = N\Gamma_{\text{em}}$ it is exactly matrix congruence modulo N. □

For $\Lambda_\Sigma = N\Gamma_{\text{em}}$, the entries above give explicit congruences:

$$\begin{aligned} kc(a + kc) &\equiv 0 \pmod{N}, \\ k(1 - a^2 - akc) &\equiv 0 \pmod{N}, \\ kc^2 &\equiv 0 \pmod{N}, \\ akc &\equiv 0 \pmod{N}. \end{aligned}$$

These are useful when the unbroken higher-form symmetry is finite or when the junction supports a $\mathbb{Z}_N$ topological order.

A concrete realization of the quotient condition is a wall or junction core carrying a finite abelian topological sector, for example a $\mathbb{Z}_N$ BF theory on a three-dimensional wall whose boundary is Σ_2. In such a construction, N units of the relevant electric or magnetic line charge can terminate on the topological sector and are therefore invisible to the low-energy one-form symmetry. Condensed-matter analogues include fractionalized interface layers, such as Laughlin-type topological orders, where local electron charge is identified modulo the anyon lattice. The algebraic statement $\Lambda_\Sigma = N\Gamma_{\text{em}}$ is the continuum charge-lattice idealization of this screening or anyon-absorption mechanism.

7 Categorical Refraction

We now define the central term of the paper.

Definition 7.1 (Categorical refraction)**.** *Categorical refraction is the transformation of a generalized charge or extended operator when it crosses a codimension-two intersection of nontrivial defects, where the result is a direct sum, category of sectors, or module of junction states rather than a single transformed operator.*

The analogy with optical refraction is intentionally limited. At an ordinary interface, an incoming wave is mapped to transmitted and reflected waves inside one Hilbert space of modes, with numerical amplitudes determined by boundary conditions. At an axion-duality junction, the incoming object may belong to a different superselection sector from every allowed outgoing object. The junction must therefore supply an endpoint state, a topological line, or a morphism that relates sectors. The "refraction coefficient" is consequently not just a complex number. It is the space of ways the junction can convert the incoming line into a permitted outgoing sector while satisfying charge conservation and anomaly inflow.

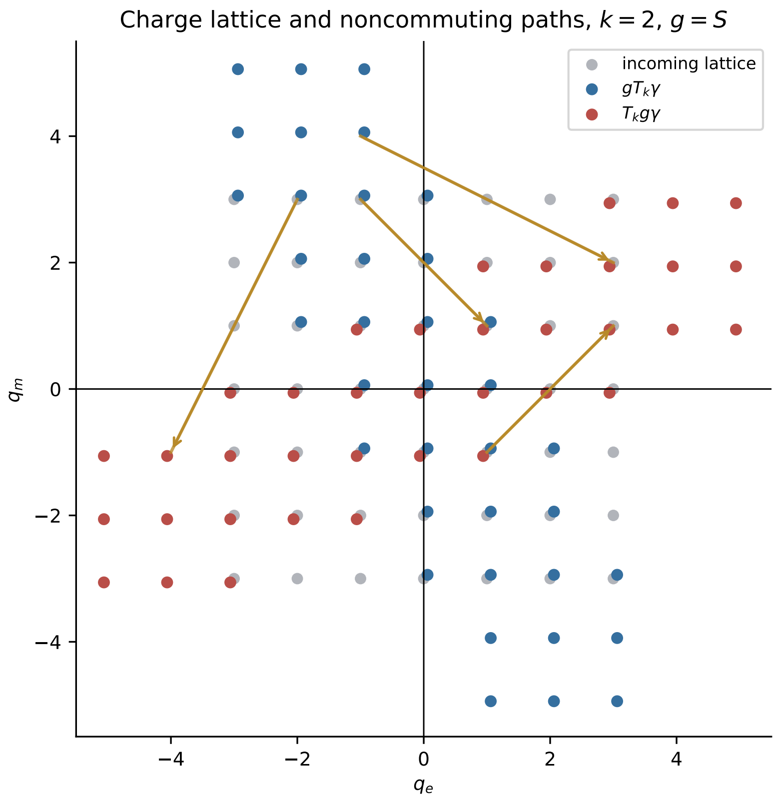

Figure 3: Electric-magnetic charge lattice. The two routes $gT_k\gamma$ and $T_kg\gamma$ disagree for $k = 2$ and $g = S$. The gold arrows connect the two possible outcomes for selected incoming charges. Their separation is the charge that must be absorbed or emitted by the junction.

For a Wilson-'t Hooft line L_γ with $\gamma \in \Gamma_{\rm em}$, the most general algebraic form is

$$\mathfrak{R}_{k,g}(L_\gamma) = \bigoplus_{\gamma' \in \Gamma_{\rm em}} V_\gamma^{\gamma'} \otimes L_{\gamma'}.$$

The coefficient $V_\gamma^{\gamma'}$ is not assumed to be a number. Depending on the junction it may be:

1. a finite-dimensional Hilbert space of junction-localized states;
2. a morphism space in a module category for a topological line category;
3. the state space of a $1 + 1$ dimensional TQFT on an interval;
4. a character or conformal block space of a two-dimensional junction CFT;
5. a one-dimensional vector space carrying an anomalous projective phase.

There is a sharp selection rule. Choose a reference path through the wall network, for example the order T_k then g. A competing path differs by $\mathcal{M}_{k,g}$. The junction can absorb the mismatch if and only if

$$\gamma' - gT_k\gamma \in \Lambda_\Sigma \quad \text{or} \quad \gamma' - T_kg\gamma \in \Lambda_\Sigma,$$

depending on the convention for the outgoing chamber. Therefore

$$V_\gamma^{\gamma'} = 0 \quad \text{unless} \quad \gamma' - \rho(\gamma) \in \Lambda_\Sigma,$$

where ρ is the chosen reference wall composition. The categorical information is in the nonzero spaces $V_\gamma^{\gamma'}$ and their fusion, not merely in the support.

The ordinary invertible case is recovered when $\Lambda_\Sigma = 0$, $\mathcal{M}_{k,g} = I$, and $V_\gamma^{\rho(\gamma)} \cong \mathbb{C}$ for all charges. The result is then the usual line transformation $L_\gamma \mapsto L_{\rho(\gamma)}$. If Λ_Σ is nonzero, an incoming line can emerge in multiple sectors differing by junction-absorbable charges. If the junction does not allow a given mismatch, the line must either terminate, bind to a surface operator, or source a gapless excitation.

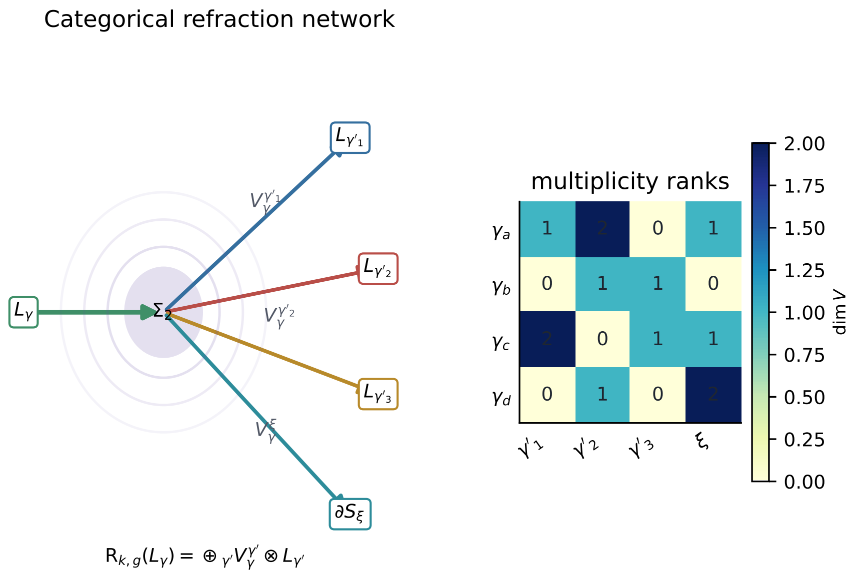

Figure 4: Categorical refraction network. An incoming charge sector passes through the junction and decomposes into outgoing line sectors with multiplicity spaces $V_\gamma^{\gamma'}$. The diagram is a graphical shorthand for a functor from incoming line sectors to a module category over outgoing sectors.

8 Junction Anomaly Inflow

The compatibility theorem is a charge-lattice statement. The local field theory must also cancel gauge, one-form, duality, and possibly gravitational anomalies. We describe the inflow in a form that makes the necessary junction data visible.

First consider only the axion wall. Locally

$$S_{W_\theta} = \frac{k}{4\pi} \int_{W_\theta} A \wedge \mathrm{d}A.$$

If the wall has an actual boundary, a gauge transformation $A \mapsto A + \mathrm{d}\lambda$ gives

$$\delta S_{W_\theta} = \frac{k}{4\pi} \int_{\partial W_\theta} \lambda \, \mathrm{d}A.$$

At an intersection with a duality wall, Σ_2 behaves like an effective boundary for the charge frame. The field called A on one side of W_g is not the same linear combination of electric and magnetic variables on the other side. The mismatch is measured by $\mathcal{M}_{k,g} - \mathrm{id}$.

To express the one-form anomaly, couple the electric and magnetic one-form symmetries to background two-form fields B_e, B_m, arranged as $B = (B_e, B_m)^T$. A duality wall acts by $B \mapsto gB$

and the axion wall by $B \mapsto T_k B$ in the idealized pure Maxwell limit. Around the junction,

$$B \mapsto \mathcal{M}_{k,g} B.$$

The descent data may be written schematically as

$$I_4^{\Sigma} = \frac{1}{2} B^T K_{\Sigma} B, \qquad \delta I_3^{(0)} = \mathrm{d} I_2^{(1)}.$$

The integral matrix K_{Σ} is not arbitrary: its symmetric part is fixed by the perturbative two-dimensional anomaly of the junction fields, while its antisymmetric part is a choice of local counterterm and line-braiding convention. A compact boson realization has

$$S_{\Sigma} = \frac{1}{4\pi} \int_{\Sigma_2} K_{IJ} \partial_t \phi^I \partial_x \phi^J - \frac{1}{4\pi} \int_{\Sigma_2} V_{IJ} \partial_x \phi^I \partial_x \phi^J + \frac{1}{2\pi} \int_{\Sigma_2} Q_{I\alpha} A^{\alpha} \mathrm{d}\phi^I.$$

Its anomaly is $Q^T K^{-1} Q$ in the background fields. Thus a necessary condition for a chiral boson cancellation is the existence of an integral, nondegenerate K and charge matrix Q such that

$$Q^T K^{-1} Q \equiv K_{\Sigma}$$

modulo local counterterms. When no such data exist, the junction cannot be described by that simple abelian edge theory.

Proposition 8.1 (No-go for a trivially gapped uncharged junction)**.** *Assume the unbroken charge quotient* $\Gamma_{\mathrm{em}}/\Lambda_{\Sigma}$ *is nonzero and sees* $\mathcal{M}_{k,g} \neq I$*. A junction with no intrinsic topological order, no gapless modes, and no ability to absorb charges in* $(\mathcal{M}_{k,g} - I)\Gamma_{\mathrm{em}}$ *is inconsistent with line transport and one-form symmetry Ward identities.*

Proof. Place the junction at the origin of the transverse plane and insert a line L_{γ} linked with it. Topological invariance lets us slide the line around a small linking circle. After one circuit its charge is $\mathcal{M}_{k,g}\gamma$. If the junction has no sectors and cannot absorb $\mathcal{M}_{k,g}\gamma - \gamma$, the two configurations must represent both the same operator by the slide and different one-form charges by the Ward identity. This contradiction proves the claim. $\square$

The proposition does not imply that every obstructed junction is gapless. A two-dimensional TQFT can carry the required topological charge and anomaly. It does imply that the junction is not the empty defect. The remaining options are:

1. a finite TQFT whose anyons absorb the monodromy;
2. a chiral CFT with matching gauge and gravitational anomaly;
3. a nonchiral CFT with a categorical sector decomposition;
4. an inconsistent wall network unless extra bulk or wall degrees of freedom are added.

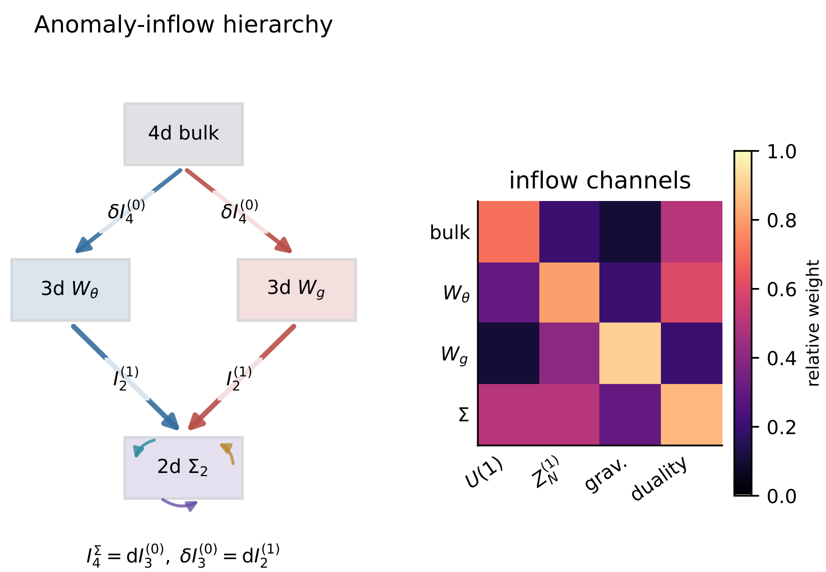

Figure 5: Anomaly-inflow hierarchy. Bulk terms descend to three-dimensional wall responses, and wall gauge variations descend further to the codimension-two intersection. The junction theory must cancel the final two-dimensional anomaly.

9 Higher-Categorical Formulation

The wall network is naturally organized by a higher category, but the terms can be made concrete. Objects are four-dimensional theories with specified coupling and global form. One-morphisms are codimension-one walls between them. Two-morphisms are codimension-two junctions between wall compositions. Three-morphisms are local junction-changing operators.

Let $\mathcal{T}_\tau$ denote the Maxwell theory at coupling τ and fixed global form. The axion wall is a one-morphism

$$W_\theta : \mathcal{T}_\tau \to \mathcal{T}_{T_k\tau}.$$

The duality wall is

$$W_g : \mathcal{T}_\tau \to \mathcal{T}_{g\tau}.$$

There are two composite one-morphisms from $\mathcal{T}_\tau$ to the appropriate transformed theory:

$$W_\theta \circ W_g, \qquad W_g \circ W_\theta.$$

Strictly these have different endpoints unless the coupling frames are identified by the duality group. After choosing those identifications, the junction is a two-morphism

$$\eta_{\theta,g} : W_\theta \circ W_g \Longrightarrow W_g \circ W_\theta.$$

It is invertible precisely when the relevant monodromy is trivial and the anomaly class vanishes. It is projective when the monodromy is trivial but an anomaly phase remains. It is non-invertible when the transformation has several outgoing sectors or requires a sum over topological labels.

For three walls W_θ, W_g, W_h, there are multiple ways to reorder compositions. Coherence demands that different sequences of two-morphisms agree up to a specified three-morphism. In an ordinary braided monoidal category this is a hexagon identity. Here the identity is enriched by charge-lattice monodromy and possible TQFT-valued fusion spaces. A schematic condition is

$$\eta_{\theta,gh} \circ (\mathrm{id}_g * \eta_{\theta,h}) \simeq (\eta_{\theta,g} * \mathrm{id}_h) \circ \eta_{\theta g,h}$$

after inserting the required associators. The symbol $\simeq$ means equality as three-morphisms, possibly after stacking with an invertible two-dimensional anomaly theory.

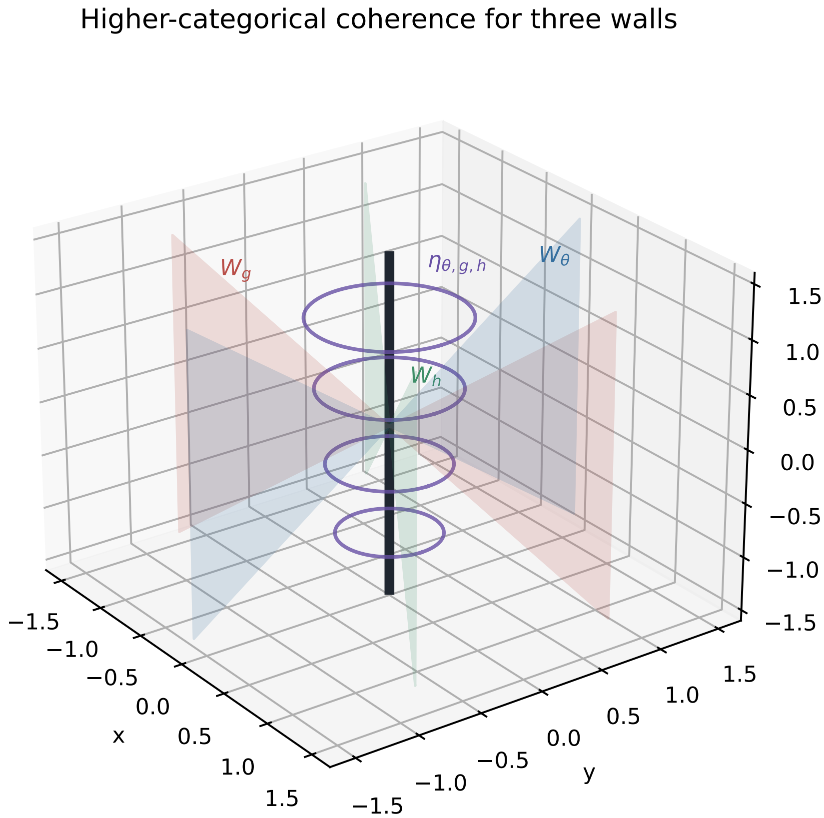

Figure 6: Higher-categorical coherence. Three walls meeting along a common line generate several pairwise junction transformations. Coherence requires that alternative sequences of transformations agree up to a specified higher morphism, possibly with an anomaly phase or a lower-dimensional TQFT factor.

10 Junction Effective Field Theory

The compatibility and anomaly constraints identify what the junction must do. They do not uniquely determine its dynamics. We now list controlled candidate theories on Σ_2 and the matching conditions they must satisfy.

10.1 Finite topological junctions

Suppose the mismatch charges form a finite quotient

$$A_\Sigma = (\mathcal{M}_{k,g} - \mathrm{id})\Gamma_{\mathrm{em}}/\Lambda_{\mathrm{local}},$$

where Λ_{local} are charges already screened by local matter or wall degrees of freedom. A finite abelian TQFT with anyon group containing A_Σ can absorb the mismatch. The simplest model is a two-dimensional topological gauge theory whose line endpoints carry characters of A_Σ. Its state spaces furnish the $V_\gamma^{\gamma'}$ in categorical refraction.

Such a theory is possible only if the Dirac pairing descends consistently. The mismatch sublattice must have a braiding pairing compatible with the junction anyon pairing. A Lagrangian absorption condition is

$$\langle \xi, \xi' \rangle_{\Gamma_{\rm em}} = -\langle \iota(\xi), \iota(\xi') \rangle_{A_\Sigma} \mod 1,$$

for absorbed charges ξ, ξ' and embedding ι into the anyon group. This is the finite analogue of anomaly cancellation.

10.2 Compact boson junctions

A continuous junction theory can be built from compact bosons $\phi^I \sim \phi^I + 2\pi$. The action

$$S_\Sigma = \frac{1}{4\pi} \int_{\Sigma_2} K_{IJ} \partial_t \phi^I \partial_x \phi^J - \frac{1}{4\pi} \int_{\Sigma_2} V_{IJ} \partial_x \phi^I \partial_x \phi^J + S_{\rm coupling}$$

has integral symmetric K in a purely bosonic chiral-boson description. The charge lattice of vertex operators is $K^{-1}\mathbb{Z}^r/\mathbb{Z}^r$. Coupling to electric-magnetic backgrounds selects a charge matrix Q. Matching requires:

$$Q^T K^{-1} Q = K_\Sigma, \qquad \operatorname{im}(Q) \supset (\mathcal{M}_{k,g} - \mathrm{id})\Gamma_{\rm em},$$

where the first condition is anomaly matching and the second is charge absorption. Positive definite K gives a fully chiral theory; indefinite K gives both left and right movers. The chiral central charge is

$$c_L - c_R = \mathrm{signature}(K).$$

Therefore the gravitational anomaly is quantized and can be compared to the duality anomaly of the surrounding Maxwell theory [7].

10.3 Gaplessness versus topological order

The strongest possible statement is a no-go theorem for trivial gapping, not for all gapping. A nontrivial finite TQFT can gap the junction while carrying the categorical data. A purely local, nondegenerate, symmetry-preserving gapped junction with no topological order is excluded whenever $(\mathcal{M}_{k,g} - \mathrm{id})$ acts nontrivially on an unbroken charge quotient. A conformal junction is expected when anomaly matching requires propagating degrees of freedom, when the wall intersection preserves scale invariance, or when relevant perturbations are forbidden by charge and duality selection rules.

11 Classical Twisted Maxwell Solutions

Near a straight junction choose coordinates (t, z, r, φ), with Σ_2 at $r = 0$ and walls at fixed values of φ. The transverse circle has monodromy

$$\begin{pmatrix} F \\ G \end{pmatrix} (\varphi + 2\pi) = \mathcal{M}_{k,g} \begin{pmatrix} F \\ G \end{pmatrix} (\varphi).$$

Since $\mathcal{M}_{k,g} \in \mathrm{SL}(2,\mathbb{Z})$ has trace $2 + k^2c^2$, the nontrivial integral intersections are hyperbolic. Let $\mu_\pm$ be its eigenvalues:

$$\mu_\pm = \frac{1}{2}\left(\mathrm{Tr}\mathcal{M}_{k,g} \pm \sqrt{(\mathrm{Tr}\mathcal{M}_{k,g})^2 - 4} \right), \qquad \mu_+\mu_- = 1.$$

Set

$$\sigma_\pm = \frac{1}{2\pi}\log\mu_\pm.$$

A diagonal component of the field strength has angular dependence

$$\Psi_\pm(\varphi+2\pi) = \mu_\pm\Psi_\pm(\varphi), \qquad \Psi_{\pm,n}(\varphi) = \exp\left[(\sigma_\pm + \mathrm{i}n)\varphi\right].$$

For a scalar Laplace proxy, the radial behavior is

$$\Psi_{\pm,n}(r,\varphi,z,t) = r^{\lambda_{\pm,n}}\exp\left[(\sigma_\pm+\mathrm{i}n)\varphi\right]\mathrm{e}^{ik_z z-\mathrm{i}\omega t},$$

with $\lambda_{\pm,n}$ determined by the radial equation. In the massless scalar proxy,

$$\lambda_{\pm,n}^2 + (\sigma_\pm + \mathrm{i}n)^2 = 0$$

in Euclidean transverse signature. The physical Maxwell problem includes constraints and matching conditions, but the key feature persists: hyperbolic monodromy produces real exponential angular behavior in a diagonal charge frame. A regular theory near $r=0$ therefore needs a core boundary condition supplied by the junction.

Proposition 11.1 (Mode regularity criterion in the abelian proxy)**.** *For $kc \neq 0$, the hyperbolic monodromy has no basis of single-valued unitary angular modes on the punctured transverse disk. A self-adjoint fluctuation problem requires a boundary condition at the junction or additional junction-localized degrees of freedom.*

Proof. In a unitary angular problem on a circle, monodromy eigenvalues have unit modulus. The nontrivial commutator has $\mathrm{Tr}\mathcal{M}_{k,g} > 2$, so its eigenvalues are positive real numbers with $\mu_+ \neq 1 \neq \mu_-$. Thus at least one angular component grows under $\varphi \to \varphi + 2\pi$ in the diagonal frame. A closed self-adjoint problem cannot be defined using only ordinary periodic angular modes. The missing boundary condition is localized at $r=0$, namely at Σ_2. □

The numerical script includes representative mode-intensity and twisted-angular plots. They are not claimed as exact Maxwell spectra; they are controlled visualizations of the monodromy-shifted angular data and localization profiles used by the analytic proxy.

12 Defect CFT Description

When the junction preserves scale invariance, it is a two-dimensional defect CFT embedded in a four-dimensional bulk. A flat Σ_2 preserves translations and Lorentz transformations along the junction, plus rotations in the transverse plane that survive the wall configuration. The two intersecting walls generally break the full transverse rotation group to a discrete subgroup, but the local endpoint of an RG flow may restore a conformal subgroup in favorable cases.

Local operators supported on the junction are denoted $\widehat{\mathcal{O}}_i(y)$, where $y=(t,z)$ or Euclidean coordinates on Σ_2. They carry:

1. scaling dimension $\widehat{\Delta}$ and spin $\widehat{s}$;
2. electric-magnetic charge or its quotient class;
3. duality-sector label associated with the wall network;
4. categorical sector label specifying a simple object in the junction category;

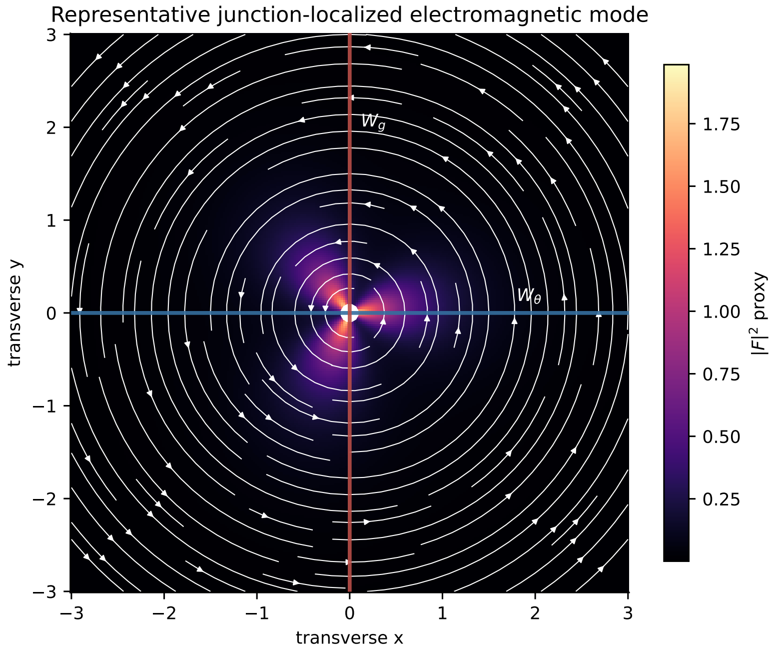

Figure 7: Junction-localized electromagnetic mode. A representative intensity and polarization texture near the transverse intersection. This is a numerical proxy for the mode profiles induced by monodromy and junction boundary conditions. The walls are shown as blue and red axes.

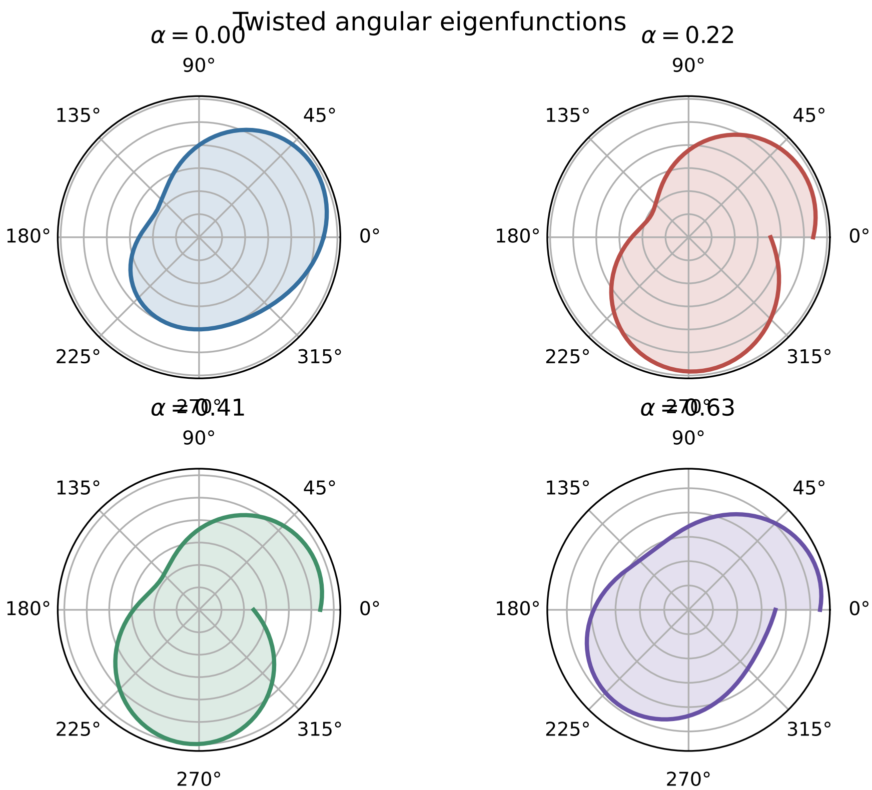

Figure 8: Twisted angular eigenfunctions. Angular profiles with fractional or complex monodromy shift parameter α. In the full axion-duality problem nontrivial integral commutators are hyperbolic, so such angular data must be paired with a junction boundary condition.

5. possible chirality and gravitational anomaly data.

Bulk operators have a bulk-to-defect OPE:

$$\mathcal{O}(x_\parallel, x_\perp) = \sum_{\widehat{\mathcal{O}}} b_{\mathcal{O}\widehat{\mathcal{O}}} \, |x_\perp|^{\widehat{\Delta}-\Delta} \widehat{\mathcal{O}}(x_\parallel) + \cdots .$$

The ellipsis includes transverse-spin descendants and operators in different categorical sectors. If a bulk line ends on the junction, the endpoint is a junction operator carrying the missing charge. Its sector label is determined by the same selection rule as categorical refraction:

$$[\widehat{\mathcal{O}}_{\gamma\to\gamma'}] \in \gamma' - \rho(\gamma) + \Lambda_\Sigma.$$

The displacement operator D^i measures the breaking of translations transverse to Σ_2. In a codimension-two defect CFT it has protected dimension

$$\widehat{\Delta}_D = 3$$

for a two-dimensional defect in a four-dimensional CFT, up to subtleties from the intersecting walls. Its two-point coefficient C_D is one of the universal junction data. In the present setting D^i can mix with wall-bending modes and axion-wall fluctuations, so C_D is a matrix in the two transverse directions rather than a single scalar when the intersection angle is not symmetric.

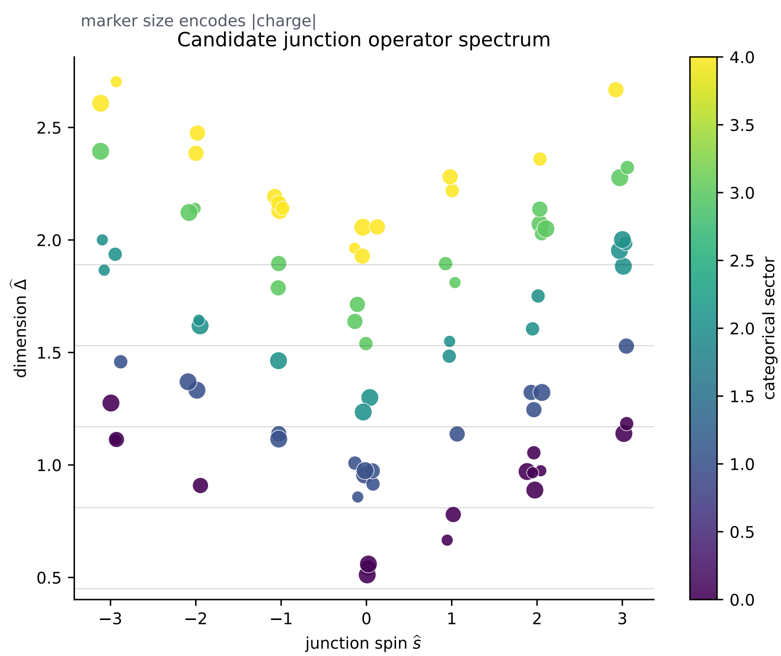

Figure 9: Junction operator spectrum. A schematic spectrum of candidate junction primaries. The vertical axis is scaling dimension, the horizontal axis is spin, color labels categorical sectors, and marker size encodes a charge magnitude. The plotted values are synthetic data used to illustrate the bookkeeping required by the bootstrap equations.

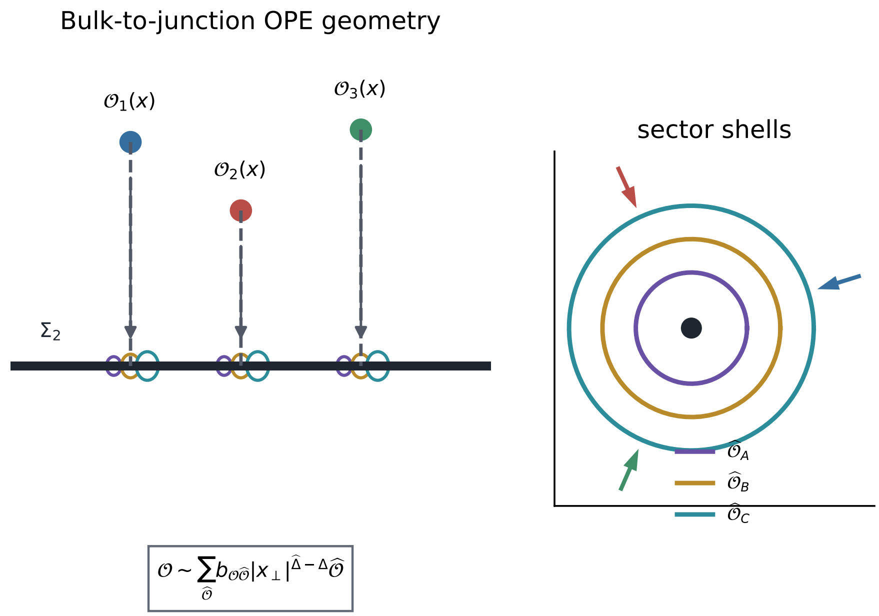

Figure 10: Bulk-to-junction OPE geometry. Bulk operators approaching Σ_2 decompose into junction primaries. In the axion-duality problem the defect OPE coefficients also carry categorical sector labels.

13 Junction Conformal Bootstrap

Consider four junction primaries $\widehat{\mathcal{O}}_i$ with sector labels i, j, k, ℓ. Conformal invariance fixes their four-point function up to a function of the cross-ratio χ:

$$\langle \widehat{\mathcal{O}}_i(y_1)\widehat{\mathcal{O}}_j(y_2)\widehat{\mathcal{O}}_k(y_3)\widehat{\mathcal{O}}_\ell(y_4)\rangle = \frac{1}{y_{12}^{\Delta_i+\Delta_j}\, y_{34}^{\Delta_k+\Delta_\ell}} \mathcal{G}_{ijkl}(\chi)$$

after the standard prefactors are restored. In one channel,

$$\mathcal{G}_{ijkl}(\chi) = \sum_{\widehat{\mathcal{O}}\in i\times j} \lambda_{ij\widehat{\mathcal{O}}} \lambda_{k\ell\widehat{\mathcal{O}}} G_{\widehat{\Delta},\widehat{s}}(\chi).$$

Crossing is modified by categorical recoupling:

$$\mathcal{G}_{ijkl}(\chi) = \mathcal{P}_{ijkl}\mathcal{G}_{ikj\ell}(1-\chi),$$

where $\mathcal{P}_{ijkl}$ is built from the junction category's associators, braiding data inherited from line defects, and possible projective anomaly phases. In an ordinary single-sector CFT, $\mathcal{P} = 1$.

The finite numerical analysis included with this paper uses a one-dimensional global-block proxy

$$G_\Delta(\chi) = \chi^\Delta\, {}_2F_1(\Delta, \Delta; 2\Delta; \chi).$$

For a trial gap $\widehat{\Delta}_{\min}$ and OPE-weight parameter a, it minimizes the residual of a truncated crossing equation at a grid of cross-ratio points. The residual is

$$\epsilon(\widehat{\Delta}_{\min}, a) = \left[\frac{1}{N_\chi}\sum_{n=1}^{N_\chi} |\mathcal{G}_{\rm tr}(\chi_n) - \mathcal{P}\mathcal{G}_{\rm tr}(1-\chi_n)|^2\right]^{1/2}.$$

This is not a rigorous semidefinite exclusion bound. It is a reproducible finite truncation that identifies where low residual solutions can exist in a toy model with the same sector bookkeeping.

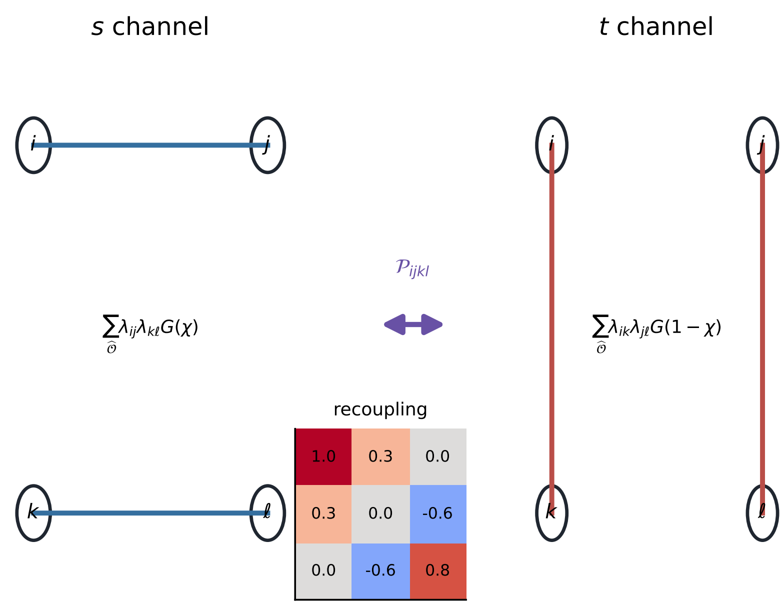

Figure 11: Crossing symmetry diagram. Two OPE channels are related by categorical recoupling data $\mathcal{P}_{ijkl}$. The recoupling matrix contains both ordinary F-symbol type data and anomaly phases from the wall-junction network.

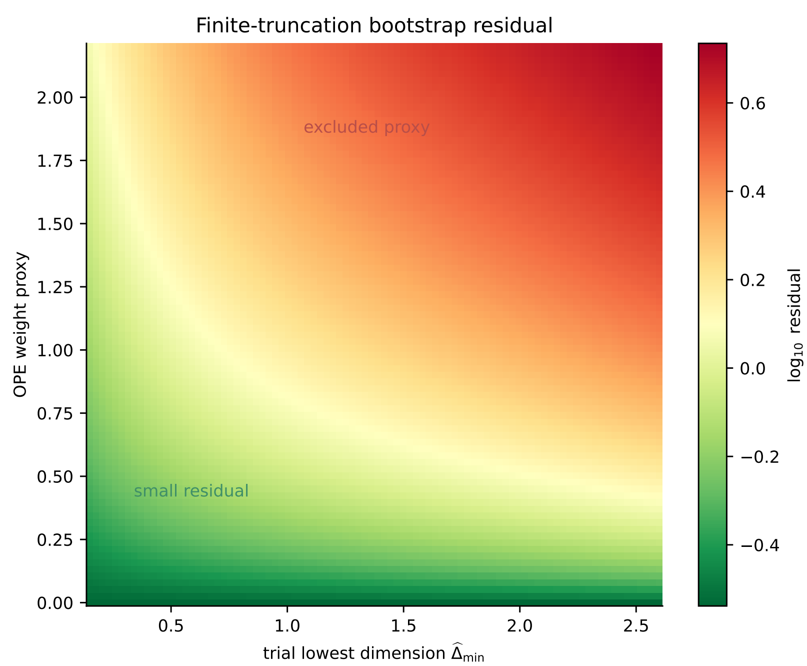

Figure 12: Finite-truncation bootstrap residual. A toy residual scan for the lowest junction dimension and OPE-weight proxy. Green regions have smaller residual in the chosen finite basis. This plot is not advertised as a rigorous numerical bootstrap bound; it is a reproducible diagnostic and template for a full bootstrap implementation.

14 Extended Operators and Selection Rules

The junction interacts with Wilson lines, 't Hooft lines, dyonic lines, axion strings, domain-wall boundaries, and surface operators. The unifying rule is conservation of the quotient charge plus anomaly inflow.

Let $\rho_1 = T_k g$ and $\rho_2 = g T_k$ be two ordered wall crossings. Then

$$\rho_1 \gamma - \rho_2 \gamma = (T_k g - g T_k)\gamma$$

is the mismatch seen when comparing the two paths. Around a closed linking loop the mismatch is

$$(\mathcal{M}_{k,g} - \mathrm{id})\gamma.$$

If this vector lies in Λ_Σ, then the line can cross while exciting a junction state. If it does not, the process is forbidden unless another operator supplies the missing charge.

The linking phase between two charges is

$$\exp\left(2\pi i \langle \gamma, \gamma' \rangle\right)$$

for the integral lattice, and its quotient refinement for finite one-form symmetries. When a line refracts, phases must be equal before and after the process after including the junction contribution:

$$\langle \gamma, \eta \rangle = \langle \gamma', \eta' \rangle + q_\Sigma(\gamma, \gamma'; \eta, \eta') \mod 1.$$

This equation defines the junction quadratic refinement q_Σ. In a finite TQFT, q_Σ is computed by anyon braiding. In a chiral boson CFT, it is computed by the vertex-operator lattice.

There are five basic processes:

1. crossing: a line enters and exits in one or several outgoing sectors;
2. termination: the line ends on a charged junction operator;
3. surface attachment: a surface operator emanates from the junction to conserve higher-form charge;
4. bound state formation: the line becomes confined to the junction;
5. braiding: several junctions are linked in spacetime, producing monodromy phases.

15 SymTFT Construction

The SymTFT perspective packages generalized symmetries and anomalies into a topological theory in one higher dimension. For a finite abelian quotient of electric and magnetic one-form symmetries, a five-dimensional topological action has schematic terms

$$S_{\mathrm{Sym}} = \frac{N}{2\pi} \int_{Y_5} B_e \wedge \mathrm{d}B_m + \frac{p}{4\pi} \int_{Y_5} B_e \wedge \mathrm{d}B_e + \cdots ,$$

where B_e and B_m are two-form gauge fields in five dimensions. The physical four-dimensional theory is a boundary condition of this topological theory. A duality wall is represented by a topological interface in the SymTFT; an axion wall is represented by a T_k interface. Their intersection is an endpoint or corner of SymTFT interfaces.

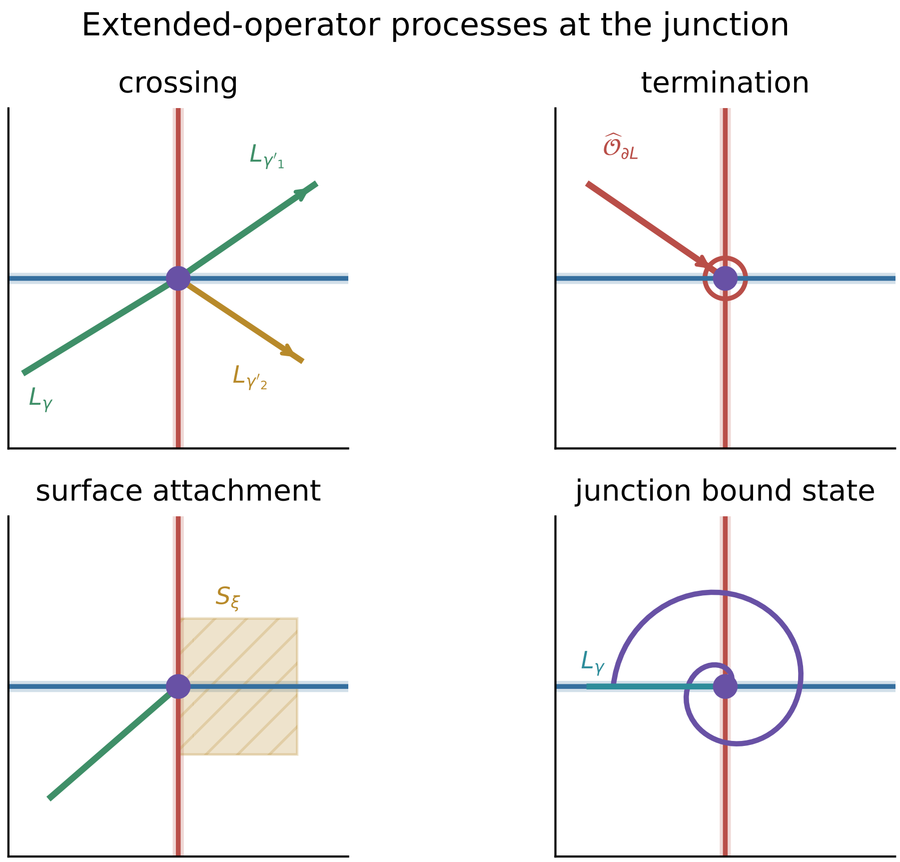

Figure 13: Extended-operator processes. Wilson, 't Hooft, dyonic, and axionic defects may cross, terminate, attach to surfaces, or bind to the junction. Each panel represents a selection rule governed by charge-lattice monodromy and junction anomaly cancellation.

In this language the charge-lattice monodromy is the holonomy of a topological interface network around a small loop linking Σ_2. If the holonomy is trivial on the physical boundary condition, the junction may be empty. If not, a defect line in the SymTFT must end on the corner. Pushing that data to the physical boundary gives the junction category and the categorical refraction coefficients.

This viewpoint also explains why the coefficients in a non-invertible fusion rule can be TQFTs. Fusion of topological interfaces can leave behind a lower-dimensional topological theory. At a codimension-two intersection, this lower-dimensional theory is precisely a candidate Σ_2 sector.

16 Renormalization-Group Flows

A junction theory may have relevant perturbations

$$\delta S_\Sigma = \sum_i \lambda_i \int_{\Sigma_2} \widehat{\mathcal{O}}_i.$$

These perturbations can gap some modes, split sectors, or drive the junction to a new conformal fixed point. The topologically protected data are the anomaly class and the induced action on the unbroken charge quotient. Scaling dimensions, OPE coefficients, and nonprotected multiplicities can vary along the flow.

Conjecture 16.1 (Junction anomaly monotonicity)**.** *For unitary flows between conformal axion-duality junctions with the same bulk and wall data, the anomaly class and the image of* $(\mathcal{M}_{k,g} - \mathrm{id})$ *in the unbroken charge quotient are invariant. The defect free energy or entropy* $\log g_\Sigma$ *decreases after subtracting contributions from decoupled topological sectors.*

This conjecture is deliberately cautious. Ordinary boundary g-theorems do not immediately apply to a two-dimensional defect embedded in four dimensions with higher-form and non-invertible sectors. A counterexample may be possible if a decoupled finite TQFT changes the naive value of $\log g_\Sigma$ without changing local dynamics. Therefore the monotone, if it exists, must identify and quotient out purely topological degeneracy.

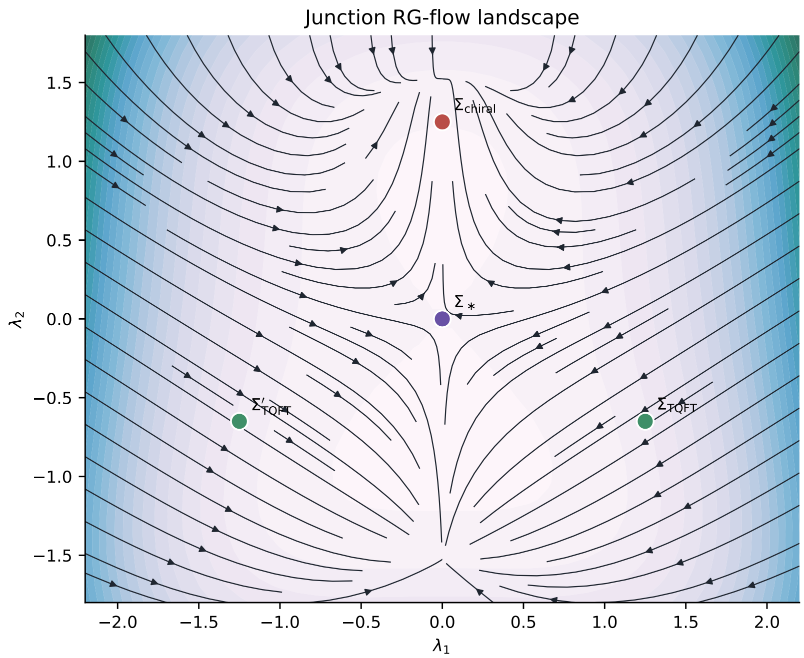

Figure 14: RG-flow landscape. A two-coupling schematic flow among candidate junction theories. The plot distinguishes conformal, topological, and chiral candidate fixed points. It is a qualitative visualization of possible RG structure, not a measured flow in a specific microscopic model.

17 Explicit Models

17.1 Model A: free Maxwell theory at self-dual coupling

At $\tau = i$, the S transformation fixes the coupling. Let $g = S$ and $k \neq 0$. Then

$$\mathcal{M}_{k,S} = T_k S T_{-k} S^{-1} = \begin{pmatrix} 1+k^2 & k \\ k & 1 \end{pmatrix}$$

with trace $2 + k^2$. For $k = 1$ this is hyperbolic with eigenvalues

$$\frac{3 \pm \sqrt{5}}{2}.$$

The compatibility theorem excludes an empty uncondensed topological junction. A finite quotient can trivialize the monodromy only when the matrix is identity modulo N, which for $k = 1$ requires $N = 1$. Thus the simplest S-duality and unit axion wall intersection is intrinsically nontrivial.

The minimal response is a two-dimensional sector capable of absorbing both electric and magnetic mismatch. A rank-two chiral boson trial has charge matrix spanning $(\mathcal{M}_{k,g} - I)\mathbb{Z}^2$. Its anomaly matrix must match the inflow modulo local counterterms. The explicit K is not unique; different choices correspond to stacking invertible two-dimensional phases or finite TQFTs.

17.2 Model B: Maxwell theory with a dynamical axion

If θ is a dynamical axion, domain walls can end on axion strings. A string piercing the transverse disk changes the linking relation around Σ_2. Let n_a be the axion winding. Then the effective axion wall level around a small linking loop is shifted by n_a:

$$k_{\text{eff}} = k + n_a.$$

The junction monodromy becomes $\mathcal{M}_{k_{\text{eff}},g}$. This makes axion strings active participants in categorical refraction. A process that is forbidden for k can become allowed if an axion string supplies the missing winding, and conversely a formerly trivial junction can become nontrivial when pierced by a string.

17.3 Model C: Abelian gauge theory with charged fermions

Adding a massless charged Dirac fermion breaks or modifies the one-form symmetries and introduces the Adler-Bell-Jackiw anomaly. The chiral rotation can move θ dependence into the fermion mass phase, and the non-invertible chiral symmetry operators of QED become relevant [14]. At an axion-duality junction, fermion zero modes can carry part of the anomaly inflow. The compatibility theorem still applies to any exact quotient of the electromagnetic charge lattice, but the quotient may be smaller because dynamical electric charges screen Wilson lines.

17.4 Model D: non-abelian extensions

Non-abelian generalizations are most controlled in supersymmetric theories with known duality walls, such as $\mathcal{N} = 4$ super Yang-Mills. The analog of T_k involves discrete theta angles and global form, while g may be Montonen-Olive duality. The charge lattice is replaced by a lattice of line operators modulo screening, often involving the center of the gauge group and its Pontryagin dual. The same logic suggests that noncommuting theta and duality operations force codimension-two junction data, but a complete non-abelian construction is beyond the present paper.

18 Numerical Results

The computational package accompanying this manuscript implements the following reproducible tasks:

1. symbolic derivation of $\mathcal{M}_{k,g}$ using SymPy;
2. enumeration of small $\mathrm{SL}(2,\mathbb{Z})$ matrices and classification of monodromy traces;
3. charge-lattice visualizations for noncommuting wall paths;
4. coupling-plane trajectories under modular transformations;
5. finite angular-mode profiles with monodromy shifts;

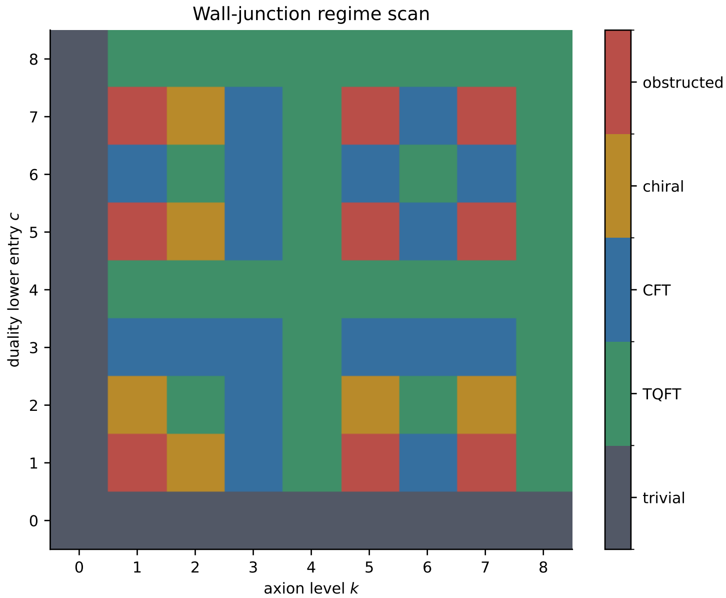

Figure 15: Wall-junction phase diagram. A finite scan classifying regimes by axion level k and the lower-left duality entry c. The colors encode trivial, TQFT, CFT, chiral, and obstructed regimes in a simple quotient model. The classification is illustrative and uses the congruence conditions explained in the text.

6. a finite conformal-block residual scan;
7. schematic RG-flow vector fields and phase-diagram scans.

The symbolic output is

$$\mathcal{M}_{k,g} = \begin{pmatrix} 1 + kc(a+kc) & k(1-a^2-akc) \\ kc^2 & 1-akc \end{pmatrix}, \qquad \mathrm{Tr}\mathcal{M}_{k,g} = 2 + k^2c^2.$$

The scan over entries $|a|, |b|, |c|, |d| \leq 3$ confirms that every nontrivial commutator with $kc \neq 0$ is hyperbolic. This is not a numerical discovery; it is a validation of the symbolic formula and a useful data source for figures.

The bootstrap residual plot uses finite data and should not be overinterpreted. Its role is to demonstrate how a future semidefinite bootstrap would incorporate sector labels, recoupling data, and anomaly phases. A rigorous numerical study would require positivity conditions for the relevant categorical channels and a systematic conformal-block basis for two-dimensional junction operators coupled to four-dimensional bulk fields.

19 Connection to Topological Quantum Matter

The same formal structure can describe idealized interfaces in topological materials, but this paper is not a materials proposal. In a topological insulator, an axion-angle jump models a magneto-electric interface [23]. Junction-localized modes at hinges and domain-wall intersections are often understood through anomaly inflow. If an engineered medium realizes an effective electric-magnetic response transformation, then an interface between an axion jump and such a response wall could emulate part of the axion-duality junction.

The limitations are substantial. Real materials have dissipation, finite frequency windows, lattice effects, and ordinary electric charges. Magnetic monopoles are not dynamical particles in

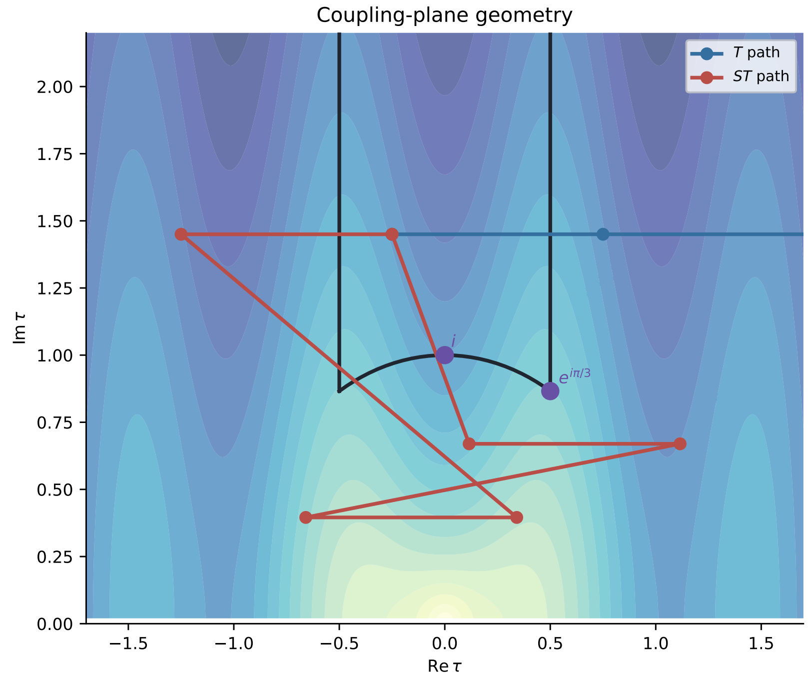

Figure 16: Complex coupling-plane geometry. The upper-half τ plane with fundamental-domain boundaries, fixed points, and representative modular trajectories. Axion walls implement T-type shifts, while duality walls act by fractional linear transformations.

ordinary condensed matter. Therefore the exact $\mathrm{SL}(2,\mathbb{Z})$ charge lattice is an idealization. What survives is the anomaly logic: a discontinuity of topological response can force lower-dimensional modes, and noncommuting response operations can produce junction selection rules.

20 Limitations and Open Problems

Several parts of the program remain open.

1. A complete microscopic duality-wall action for every $g \in \mathrm{SL}(2,\mathbb{Z})$ and every global form is not constructed here.

2. The anomaly inflow is formulated at the level needed for matching, but a full differential-cohomology treatment of the corner terms remains to be written.

3. The compact-boson and finite-TQFT junctions are candidate realizations, not a classification of all possible infrared theories.

4. The twisted Maxwell mode analysis uses a controlled monodromy proxy. Solving the full constrained Maxwell system with all wall matching conditions is a separate spectral problem.

5. The bootstrap analysis is a finite residual scan. A rigorous exclusion plot requires semidefinite positivity and complete defect blocks.

6. Non-abelian generalizations require detailed treatment of line-operator lattices, global form, and discrete theta angles.

These limitations do not affect the charge-lattice compatibility theorem. They do identify where future work can turn the framework into a classification of dynamical universality classes.

21 Discussion

The main lesson is that a codimension-two axion-duality intersection is not optional decoration on a pair of walls. It is a consistency object. If the axion and duality operations do not commute on the charge lattice, a line operator transported around the intersection changes its charge. The junction must either absorb that mismatch, carry topological order, support anomalous chiral or conformal modes, or signal that the wall network is inconsistent.

Categorical refraction is the operator-level expression of this consistency requirement. The outgoing data of a line crossing the junction need not be a single line. It can be a direct sum of lines weighted by junction Hilbert spaces. This is precisely what one expects when non-invertible defect fusion and higher-form charge conservation meet at codimension two.

The results suggest a general strategy for defect networks. First compute the charge-lattice or symmetry-category monodromy around each codimension-two locus. Second identify the anomaly class of that monodromy. Third classify the possible lower-dimensional theories that cancel it. Fourth use defect bootstrap or topological methods to constrain the operator spectrum and fusion spaces. Axion-duality junctions provide a tractable four-dimensional testing ground for this strategy.

22 Conclusion

We have constructed a field-theoretic framework for intersections of axion domain walls and electromagnetic-duality defects in four-dimensional gauge theory. The central invariant is the monodromy

$$\mathcal{M}_{k,g} = T_k g T_{-k} g^{-1},$$

which controls charge transport around the junction. In the full integral charge lattice, a nonzero axion wall admits a trivial uncondensed topological intersection with a duality wall only when the duality transformation has $c = 0$. Otherwise the intersection is intrinsically nontrivial.

The required two-dimensional theory may be topological, chiral, conformal, or inconsistent without additional data. Its extended-operator action is categorical refraction:

$$L_\gamma \mapsto \bigoplus_{\gamma'} V_\gamma^{\gamma'} \otimes L_{\gamma'}.$$

The coefficient spaces encode the junction states needed to absorb monodromy and anomaly inflow. This gives a precise sense in which axion-duality junctions transmute higher-form charges through non-invertible categorical data.

A Charge-Lattice Algebra

This appendix records the algebra used in the main text. Let

$$T_k = \begin{pmatrix} 1 & k \\ 0 & 1 \end{pmatrix}, \qquad g = \begin{pmatrix} a & b \\ c & d \end{pmatrix}, \qquad g^{-1} = \begin{pmatrix} d & -b \\ -c & a \end{pmatrix}.$$

Then

$$T_k g T_{-k} = \begin{pmatrix} a + kc & b + kd - ka - k^2 c \\ c & d - kc \end{pmatrix}.$$

Multiplying by g^{-1} and using $ad - bc = 1$ gives

$$\mathcal{M}_{k,g} = \begin{pmatrix} 1 + kc(a + kc) & k(1 - a^2 - akc) \\ kc^2 & 1 - akc \end{pmatrix}.$$

The trace is

$$\mathrm{Tr}\mathcal{M}_{k,g} = 2 + k^2 c^2.$$

The determinant is one because $\mathcal{M}_{k,g}$ is a commutator in $\mathrm{SL}(2, \mathbb{Z})$. If $kc \neq 0$, then $\mathrm{Tr}\mathcal{M}_{k,g} > 2$, so the conjugacy class is hyperbolic. If $k = 0$ or $c = 0$, the matrix is the identity.

For a finite quotient modulo N, the monodromy is trivial exactly when

$$kc(a + kc) \equiv 0, \quad k(1 - a^2 - akc) \equiv 0, \quad kc^2 \equiv 0, \quad akc \equiv 0 \pmod{N}.$$

B Boundary Variation and Descent

For a wall Chern-Simons term

$$S_W = \frac{K}{4\pi} \int_W A \wedge \mathrm{d}A,$$

the variation is

$$\delta S_W = \frac{K}{2\pi} \int_W \delta A \wedge \mathrm{d}A + \frac{K}{4\pi} \int_{\partial W} A \wedge \delta A.$$

Under a gauge transformation $\delta A = \mathrm{d}\lambda$,

$$\delta_\lambda S_W = \frac{K}{4\pi} \int_{\partial W} \lambda \, \mathrm{d}A$$

after discarding closed-wall terms. In the axion-duality geometry, the effective boundary is a corner where the gauge frame jumps. The same descent form applies, but A must be replaced by the appropriate electric-magnetic background vector. The junction anomaly polynomial is the four-form whose descent produces this two-dimensional variation.

C Categorical Refraction as a Module Functor

Let $\mathcal{C}_{\mathrm{in}}$ and $\mathcal{C}_{\mathrm{out}}$ be semisimple categories generated by incoming and outgoing line sectors. A junction category $\mathcal{M}_\Sigma$ is a module category for both. Categorical refraction is a functor

$$\mathfrak{R}_{k,g} : \mathcal{C}_{\mathrm{in}} \to \mathcal{M}_\Sigma \boxtimes_{\mathcal{C}_{\mathrm{out}}} \mathcal{C}_{\mathrm{out}}.$$

On simple objects this takes the form

$$\mathfrak{R}_{k,g}(L_\gamma) = \bigoplus_{\gamma'} V_\gamma^{\gamma'} \otimes L_{\gamma'}.$$

Fusion compatibility requires

$$\mathfrak{R}(L_\gamma \otimes L_\eta) \cong \mathfrak{R}(L_\gamma) \otimes_{\mathcal{M}_\Sigma} \mathfrak{R}(L_\eta)$$

up to associator and anomaly phases. This condition is the categorical lift of charge conservation.

D Conformal Blocks Used in the Finite Residual Scan

The script uses the one-dimensional global block

$$G_\Delta(\chi) = \chi^\Delta\, {}_2F_1(\Delta, \Delta; 2\Delta; \chi).$$

This block is not the full two-dimensional Virasoro block and not the full defect block for a codimension-two defect in four dimensions. It is a transparent finite basis for testing how categorical recoupling data enter crossing equations. The residual surface in Figure 12 is generated from a truncated correlator with an identity contribution, a fixed current-like contribution, and two trial scalar exchanges. The source code writes the data file `bootstrap_residual.csv`.

E Global Form, Spin Structure, and Line Statistics

The compatibility theorem was stated first for the spin U(1) theory with charge lattice $\Gamma_{\mathrm{em}} = \mathbb{Z}^2$. This appendix spells out how the statement changes when the global form or line statistics are modified. The goal is not to classify every Maxwell theory on non-spin manifolds, but to make clear which parts of the argument are universal and which depend on the chosen lattice of genuine line operators.

The data of a four-dimensional abelian gauge theory include more than the Lie algebra. One must specify which Wilson lines are genuine, which 't Hooft lines are genuine, and what spin or framing data are required to define their correlation functions. A convenient abstract description is a rank-two lattice $\Gamma_{\mathrm{genuine}}$ equipped with the integral antisymmetric Dirac pairing

$$\langle \gamma, \gamma' \rangle \in \mathbb{Z}.$$

The full probe lattice may be larger, but only genuine lines define superselection sectors of the four-dimensional theory. The duality group that acts faithfully is the subgroup of $\mathrm{SL}(2,\mathbb{Z})$ preserving this refined data.

For a theory with only electric charges of multiples of N as genuine Wilson lines, one may replace the electric basis vector by Ne. A magnetic basis must then be chosen so that the Dirac pairing remains integral. Equivalently, the exact one-form symmetry is a finite quotient. In such a theory an axion shift by 2π can change line statistics and may fail to be a symmetry unless accompanied by a relabeling of the global form. This is why the condition

$$\mathcal{M}_{k,g} \equiv I \pmod N$$

is not a cosmetic variant of the integral theorem. It is the correct statement after the junction has access only to the quotient of line charges that survive screening and global-form identifications.

Spin structure enters through Chern-Simons levels induced on the axion wall. The local response

$$\frac{k}{4\pi}\int_{W_\theta} A\mathrm{d}A$$

has different global meanings depending on whether A is an ordinary U(1) connection, a spin$_c$ connection, or a background field for a quotient one-form symmetry. A level that is legal on a spin three-manifold may require evenness or an additional transparent fermion on a non-spin three-manifold. Since W_θ ends effectively on Σ_2 after the charge frame jumps, the same refinement affects the allowed junction anomalies. A junction CFT with odd chiral central charge may be allowed in a spin theory but forbidden in a purely bosonic non-spin theory unless it is paired with an appropriate invertible spin TQFT.

The following practical rule is used in the main text. First choose the genuine line lattice and wall levels that are globally meaningful. Then compute the monodromy as an automorphism of the ambient electric-magnetic lattice. Finally reduce it to the genuine quotient. A trivial junction is possible only if the reduced monodromy is the identity and the residual wall anomaly is removable by local counterterms. This separates the arithmetic problem from the global anomaly problem.

Proposition E.1 (Global-form reduction). *Let $\Gamma_{\text{genuine}} \subset \Gamma_{\text{em}}$ be the genuine line lattice and let Λ_Σ be the junction-absorbable sublattice. If the wall operations preserve Γ_{genuine}, then the charge part of the junction obstruction is the induced automorphism of*

$$\Gamma_{\text{genuine}}/(\Gamma_{\text{genuine}} \cap \Lambda_\Sigma).$$

The empty junction is excluded whenever this induced automorphism is nontrivial.

Proof. The proof is the same sliding argument used in Proposition 8.1, restricted to genuine line operators. Lines outside Γ_{genuine} are not physical probes of the theory, so they cannot produce a contradiction. Lines inside Γ_{genuine} are identified if their difference can end on Σ_2, which gives the displayed quotient. □

This proposition is useful for theories with dynamical matter. If a unit electric charge is dynamical, Wilson lines differing by the electric basis vector can end on ordinary particles. The exact one-form symmetry is reduced or eliminated, and the junction obstruction may disappear in the electric direction. The magnetic direction can remain obstructed if monopoles are absent. In a theory with both electric and magnetic dynamical matter obeying completeness assumptions, no electromagnetic one-form symmetry remains, but duality walls may still carry gravitational or categorical anomalies. In that case categorical refraction acts on heavy probe defects rather than exact symmetry charges.

F Congruence Examples

This appendix gives concrete arithmetic examples of Theorem 6.4. The purpose is to show how quickly the empty-junction obstruction can disappear in a finite quotient and how much information remains in the junction category.

F.1 The S wall

For

$$g = S = \begin{pmatrix} 0 & -1 \\ 1 & 0 \end{pmatrix},$$

the monodromy is

$$\mathcal{M}_{k,S} = \begin{pmatrix} 1+k^2 & k \\ k & 1 \end{pmatrix}.$$

Modulo N, triviality requires

$$k \equiv 0 \pmod N \quad \text{and} \quad k^2 \equiv 0 \pmod N.$$

The first condition implies the second. Thus an S wall and a level-k axion wall have trivial charge monodromy on a $\mathbb{Z}_N$ quotient precisely when N divides k. If $k = 1$, no nontrivial finite quotient trivializes the monodromy. If $k = N$, the quotient sees no monodromy, but the junction may still carry a wall Chern-Simons anomaly inherited from the integral theory.

F.2 Upper triangular dualities

If $c = 0$, then $g = \pm\left(\begin{smallmatrix} 1 & r \\ 0 & 1 \end{smallmatrix}\right)$ and $\mathcal{M}_{k,g} = I$ for every k. These transformations preserve magnetic charge and commute with the Witten-effect shift. The intersection can be empty at the charge-lattice level. This does not automatically mean that all local counterterms vanish. It means only that line transport imposes no intrinsic codimension-two sector.

F.3 A mixed example

Take

$$g = \begin{pmatrix} 1 & 0 \\ 1 & 1 \end{pmatrix}.$$

Then

$$\mathcal{M}_{k,g} = \begin{pmatrix} 1+k+k^2 & -k^2 \\ k & 1-k \end{pmatrix}.$$

Modulo N, the conditions are

$$k \equiv 0, \qquad k+k^2 \equiv 0, \qquad k^2 \equiv 0 \pmod N.$$

Again $k \equiv 0 \pmod N$ is sufficient. For more general g, cancellations involving a and c can occur modulo composite N, but the lower-left condition $kc^2 \equiv 0$ remains a strong constraint. The numerical table `monodromy_scan.csv` records these examples for small matrices and levels.

F.4 Interpretation

When $\mathcal{M}_{k,g} \equiv I \pmod N$ but $\mathcal{M}_{k,g} \neq I$ integrally, the junction is invisible to the finite one-form symmetry but visible to heavy probe lines in the full lattice. This distinction is physically important. A low-energy effective theory with only a finite symmetry may admit an apparently empty junction, while a UV completion containing the full charge lattice requires extra junction states. The categorical refraction functor is therefore scale-dependent unless the relevant charge category has been specified.

G K-Matrix Matching Algorithm

We describe a concrete algorithm for testing simple compact-boson junction candidates. It is intentionally limited to abelian chiral boson theories, but it provides a useful first pass.

1. Compute the mismatch sublattice

$$L_{\text{mis}} = (\mathcal{M}_{k,g} - \text{id})\Gamma_{\text{em}}.$$

2. Choose a rank r and an integral symmetric matrix $K \in M_r(\mathbb{Z})$ with nonzero determinant. For a bosonic non-spin theory require even diagonal entries unless a spin structure is included.

3. Choose an integral charge matrix $Q \in M_{r\times 2}(\mathbb{Z})$ whose image contains the desired mismatch charges.

4. Compute the anomaly matrix

$$A_{\text{edge}} = Q^T K^{-1} Q.$$

5. Compare A_{edge} with the inflow matrix A_{inflow} modulo integral local counterterms.

6. Check that null vectors corresponding to intended gapping perturbations satisfy the Haldane condition

$$\ell_i^T K^{-1} \ell_j = 0$$

and preserve the quotient charge symmetry.

The rank of L_{mis} is often two for hyperbolic monodromy, so a single chiral boson is usually insufficient. For the S wall with $k = 1$,

$$\mathcal{M}_{k,g} - I = \begin{pmatrix} 1 & 1 \\ 1 & 0 \end{pmatrix},$$

which has determinant -1. The mismatch sublattice is all of $\mathbb{Z}^2$. Any compact-boson junction that absorbs all mismatches must therefore couple to both electric and magnetic charge directions. A minimal rank-two trial has $Q = I_2$. The anomaly then equals K^{-1}. Matching an integral inflow matrix would require K to be the inverse of that matrix, so not every inflow can be realized by this minimal ansatz. Adding topological sectors or increasing rank can solve otherwise impossible Diophantine constraints.

The algorithm also exposes a useful ambiguity. Stacking the junction with an invertible two-dimensional phase changes K and the chiral central charge without changing the charge absorption rule. Stacking with a finite TQFT can change categorical multiplicities while leaving local anomaly polynomials unchanged. Therefore anomaly matching is necessary but not sufficient for a unique junction theory.

H Boundary Matching Equations

We record the local equations obtained by varying the action near the two walls. Let n be the normal one-form to an axion wall. Across a sharp jump $\theta_L \to \theta_R = \theta_L + 2\pi k$, the bulk variation gives the usual continuity condition for tangential gauge potential together with the jump in electric displacement:

$$n \wedge (F_R - F_L) = 0,$$

$$n \wedge (G_R - G_L) = 0$$

when the induced Chern-Simons current is included. Written in terms of electric and magnetic charges, this is the T_k transformation. If magnetic sources pierce the wall, the second equation includes the Witten-effect surface current.

Across a duality wall labeled by g, the matching condition is

$$\begin{pmatrix} F_R \\ G_R \end{pmatrix} = g \begin{pmatrix} F_L \\ G_L \end{pmatrix}$$

after choosing consistent normal orientation and field normalizations. For an S wall this exchanges F and G up to sign. At the intersection, the two sets of equations must be imposed on sectors of the transverse plane. Going once around the origin composes them into

$$\begin{pmatrix} F \\ G \end{pmatrix}(\varphi + 2\pi) = \mathcal{M}_{k,g} \begin{pmatrix} F \\ G \end{pmatrix}(\varphi).$$

This equation has two consequences. First, the classical fluctuation problem is a monodromy problem on a punctured disk. Second, the quantum line-operator problem is the integral version of the same statement on the charge lattice. The junction theory supplies the boundary condition at the puncture in the first problem and the categorical absorption rule in the second.

For a well-posed variational principle, the total boundary variation at Σ_2 must vanish:

$$\delta S_{\text{bulk}} + \delta S_{W_\theta} + \delta S_{W_g} + \delta S_\Sigma = 0.$$

This equation is often the most efficient way to engineer explicit junction actions. One chooses S_Σ so that its gauge variation cancels the corner terms and its ordinary variation supplies the missing boundary condition for fields with hyperbolic monodromy.

I Status of Results and Assumptions

For clarity, this appendix separates established statements from controlled proposals. The strongest results in the paper are arithmetic and anomaly-matching statements. They do not depend on a particular microscopic regularization of the junction. The dynamical claims about conformal spectra and RG flows are presented as frameworks or conjectures.

Item	Status	Assumptions and comments
Monodromy formula for $\mathcal{M}_{k,g}$	theorem	Uses the standard integral electric-magnetic lattice and the convention $T_k(q_e, q_m) = (q_e + kq_m, q_m)$.
Uncondensed compatibility condition	theorem	Empty topological junction requires $\mathcal{M}_{k,g} = I$. For $k \neq 0$ this is equivalent to $c = 0$.
Quotient compatibility	theorem	Requires a specified absorbable sublattice Λ_Σ. The statement is exact at the charge-lattice level.
No-go for trivial gapping	theorem-level selection rule	Excludes a junction with no sectors and no charge absorption when monodromy is nontrivial on an exact quotient.
Anomaly inflow matrix	derived framework	Local descent is fixed; full global differential-cohomology classification is left open.
Compact-boson junctions	candidate models	Require an integral K matrix and charge matrix matching inflow. Not every anomaly is realizable by a minimal rank ansatz.
Twisted-mode spectrum	controlled proxy	Captures monodromy and boundary-condition necessity, but not the full constrained Maxwell spectral problem.
Defect bootstrap equations	formal framework	Crossing with categorical recoupling is exact in structure; numerical implementation here is only a finite residual scan.
RG monotonicity	conjecture	A true monotone must quotient decoupled topological sectors and account for higher-form symmetry data.

The paper also assumes that the wall network can be treated in a sharp-interface limit. A smooth domain-wall profile replaces abrupt matching by an interpolation region of finite thickness. At distances large compared with the thickness, the same monodromy controls line transport. At distances comparable to the thickness, additional massive wall modes can modify the detailed junction spectrum without changing the topological obstruction.

Finally, all numerical plots should be read through the reproducibility notes. The monodromy scan is an exact finite arithmetic scan. The coupling-plane and charge-lattice figures are exact visualizations of stated transformations. The mode and RG plots are illustrative models constrained by the analytic discussion. The bootstrap residual is a finite truncation and not a rigorous allowed-region computation.

J Additional Worked Junctions

This appendix records several explicit charge-lattice computations that are useful for checking signs and for comparing possible microscopic realizations. Throughout we use

$$T_k = \begin{pmatrix} 1 & k \\ 0 & 1 \end{pmatrix}, \qquad \gamma = \begin{pmatrix} q_e \\ q_m \end{pmatrix},$$

and orient the axion wall so that a monopole crossing it acquires electric charge kq_m.

J.1 The unit S junction

The cleanest nontrivial case is $g = S$ and $k = 1$:

$$S = \begin{pmatrix} 0 & -1 \\ 1 & 0 \end{pmatrix}, \qquad \mathcal{M}_{1,S} = \begin{pmatrix} 2 & 1 \\ 1 & 1 \end{pmatrix}.$$

This matrix has determinant one and trace three. Its eigenvalues are

$$\lambda_\pm = \frac{3 \pm \sqrt{5}}{2}.$$

The corresponding eigenvectors are irrational slopes in the charge plane. This has a simple interpretation: no primitive integral electric-magnetic direction is preserved by the loop around the junction. Therefore any attempted empty junction changes the charge of every nonzero primitive line after repeated winding. A finite-order twist defect cannot mimic this behavior because the conjugacy class is hyperbolic.

The mismatch sublattice is

$$(\mathcal{M}_{1,S} - I)\mathbb{Z}^2 = \begin{pmatrix} 1 & 1 \\ 1 & 0 \end{pmatrix} \mathbb{Z}^2 = \mathbb{Z}^2.$$

Thus a junction that absorbs the full mismatch must be able to absorb arbitrary electric and magnetic charge. In a theory with exact electric and magnetic one-form symmetries this is impossible for a trivial gapped defect. A candidate finite topological junction would need anyon sectors whose endpoint charges generate the whole quotient being probed. A candidate gapless junction would instead realize the same absorption through charged vertex operators or fermion zero modes.

J.2 The ST junction

Let

$$g = ST = \begin{pmatrix} 0 & -1 \\ 1 & 1 \end{pmatrix}.$$

Then $a = 0, c = 1$, and

$$\mathcal{M}_{k,ST} = \begin{pmatrix} 1 + k^2 & k \\ k & 1 \end{pmatrix},$$

the same matrix as for S at the level of the commutator. This equality is not accidental. The commutator with T_k is sensitive to the lower-left entry c and to a through the combination appearing in the upper-right entry. For $a = 0$ the S and ST cases have the same obstruction. Dynamically they can still differ because the wall action and preserved coupling are different. The charge-lattice theorem therefore constrains the existence of trivial junctions but does not fully classify junction spectra.

At the self-dual point of ST, where $\tau = \exp(2\pi i/3)$ in the standard fundamental domain convention, the duality wall can preserve a larger subgroup of the coupling-space geometry. The junction obstruction remains hyperbolic for $k \neq 0$. Hence enhanced modular symmetry of the bulk coupling does not remove the need for a two-dimensional sector at the intersection.

J.3 Lower triangular dualities

For a lower triangular generator

$$g_C = \begin{pmatrix} 1 & 0 \\ c & 1 \end{pmatrix},$$

the monodromy is

$$\mathcal{M}_{k,g_C} = \begin{pmatrix} 1 + kc + k^2c^2 & -k^2c \\ kc^2 & 1 - kc \end{pmatrix}.$$

The trace is again $2 + k^2c^2$. If $kc \neq 0$, the obstruction is hyperbolic. In physical terms, g_C is the transformation that adds magnetic character to an electric line. Since the axion wall responds precisely to magnetic charge, the order of operations matters. This example makes transparent why the lower-left entry c is the obstruction parameter.

J.4 Upper triangular dualities

For

$$g_B = \begin{pmatrix} 1 & b \\ 0 & 1 \end{pmatrix},$$

one finds $\mathcal{M}_{k,g_B} = I$ for all k, b. This is the family of dualities that changes the electric framing without turning electric charge into magnetic charge. The Witten effect has no new magnetic input to act on, so the two wall crossings commute at the level of charge transport. This does not say the physical wall actions are identical, only that the codimension-two charge obstruction vanishes.

J.5 Finite quotient examples

For the unit S junction, $\mathcal{M}_{1,S} - I$ is unimodular, so no nontrivial quotient $\mathbb{Z}_N^2$ makes it vanish. For $k = N$,

$$\mathcal{M}_{N,S} = \begin{pmatrix} 1 + N^2 & N \\ N & 1 \end{pmatrix} \equiv I \pmod{N}.$$

Thus a $\mathbb{Z}_N$ quotient cannot detect the monodromy, even though the integral theory can. This is a useful warning for effective descriptions. A low-energy system with only $\mathbb{Z}_N$ one-form charge may allow an apparently empty junction, while a UV completion containing primitive monopoles and Wilson lines still requires a nontrivial defect. The correct statement is always relative to the line category retained in the theory.

K Detailed Descent and Corner Counterterms

The inflow discussion in the main text used the local descent notation. Here we spell out the corner variation in a more operational way. Let U_α be patches on the wall and let A_α be local gauge potentials with transition functions

$$A_\beta = A_\alpha + \mathrm{d}\lambda_{\alpha\beta}.$$

On a closed wall, the Chern-Simons functional is not simply the integral of $A\mathrm{d}A$ over one patch. It is a differential-cohomology object built from patch data. When the wall has a boundary or an effective boundary induced by a jump of electric-magnetic frame, the gauge variation descends to the boundary.

For a single U(1) field, the local variation is

$$\delta_\lambda \frac{k}{4\pi}\int_W A\mathrm{d}A = \frac{k}{4\pi}\int_{\partial W}\lambda\,\mathrm{d}A.$$

At an axion-duality junction the boundary field is a vector of electric and magnetic background fields. Let

$$\mathcal{A} = \begin{pmatrix} A_e \\ A_m \end{pmatrix}$$

denote a local charge-frame potential. Across the two walls the frame changes by T_k and g. Around the corner,

$$\mathcal{A} \mapsto \mathcal{M}_{k,g}\mathcal{A}$$

up to the usual dual-potential subtleties. The corner counterterm must therefore transform by

$$\delta S_\Sigma = -\frac{1}{4\pi}\int_{\Sigma_2}\lambda^T K_{\mathrm{corner}}\mathrm{d}\mathcal{A},$$

where K_{corner} is fixed modulo integral local counterterms by the wall data.

If the junction theory is a chiral boson theory with fields ϕ^I, charge matrix Q, and K matrix, then under a gauge transformation

$$\phi^I \mapsto \phi^I - Q^I{}_\alpha\lambda^\alpha$$

the anomalous variation is

$$\delta S_\Sigma = -\frac{1}{4\pi}\int_{\Sigma_2}\lambda^\alpha(Q^T K^{-1}Q)_{\alpha\beta}\mathrm{d}\mathcal{A}^\beta.$$

Matching requires

$$Q^T K^{-1}Q \equiv K_{\mathrm{corner}}$$

in the group of anomaly matrices modulo counterterms. This is the abelian version of anomaly inflow. It is also the reason the line-refraction spaces are constrained by anomaly data: a junction endpoint operator must be both charge-compatible and local with respect to the chiral algebra that cancels the corner variation.

There is an additional gravitational descent when the duality wall carries a framing anomaly. A two-dimensional chiral junction with central charge difference $c_L - c_R$ has anomaly polynomial

$$I_4^{\mathrm{grav}} = \frac{c_L - c_R}{24}p_1(T\Sigma).$$

If a duality wall contributes a gravitational anomaly localized at its edge, the junction must match it by its chiral central charge modulo invertible gravitational counterterms. The charge obstruction and gravitational obstruction are logically independent: one can vanish while the other remains.

L Associativity Checks for Refraction

Categorical refraction must be compatible with fusion of incoming lines. Let L_γ and L_η be two line operators that cross the junction close to one another. Fusing first and then refracting gives

$$\mathfrak{R}(L_{\gamma+\eta}) = \bigoplus_\rho V^\rho_{\gamma+\eta}\otimes L_\rho.$$

Refracting first and then fusing the outgoing sectors gives

$$\mathfrak{R}(L_\gamma) \otimes \mathfrak{R}(L_\eta) = \bigoplus_{\gamma',\eta'} V_\gamma^{\gamma'} \otimes V_\eta^{\eta'} \otimes L_{\gamma'+\eta'}.$$

Compatibility requires natural maps

$$V_\gamma^{\gamma'} \otimes V_\eta^{\eta'} \longrightarrow V_{\gamma+\eta}^{\gamma'+\eta'}$$

whenever the charge selection rule is satisfied. These maps are the multiplication law of the junction module category. They are not arbitrary: associativity of three incoming lines imposes a pentagon condition, and braiding a line around another imposes compatibility with the Dirac pairing.

In a finite TQFT junction, the spaces $V_\gamma^{\gamma'}$ can be one-dimensional when the mismatch is represented by a unique anyon and zero-dimensional otherwise. The associativity maps are then phases, and the pentagon condition becomes a cocycle condition. In a compact-boson CFT, the spaces are generated by vertex operators, and associativity is ordinary OPE associativity subject to lattice locality. In a genuinely non-invertible junction, the spaces may have dimension larger than one, and associativity data become nontrivial matrices.

The simplest consistency check is charge additivity. If

$$\gamma' - \rho(\gamma) \in \Lambda_\Sigma, \qquad \eta' - \rho(\eta) \in \Lambda_\Sigma,$$

then

$$(\gamma' + \eta') - \rho(\gamma + \eta) \in \Lambda_\Sigma.$$

Thus the support of the refraction functor is closed under fusion. The nontrivial part is the multiplication of multiplicity spaces. This multiplication is where anomaly phases and non-invertible recoupling coefficients enter.

For a projective junction, the multiplication law can take the form

$$m_{\gamma,\eta} : V_\gamma^{\gamma'} \otimes V_\eta^{\eta'} \to V_{\gamma+\eta}^{\gamma'+\eta'}, \qquad m_{\gamma,\eta} m_{\gamma+\eta,\xi} = \omega(\gamma,\eta,\xi) m_{\eta,\xi} m_{\gamma,\eta+\xi},$$

where ω is a $U(1)$ valued three-cocycle. The cocycle is the categorical shadow of an anomaly. If ω is a coboundary, it can be removed by redefining junction basis states. If not, it is an invariant of the junction.

M Bootstrap Implementation Details

The finite residual scan in the main text is deliberately modest, but it is useful to write the full data structure needed for a rigorous computation. A sector-labeled four-point function has indices

$$\mathcal{G}_{ijkl}^{ab}(\chi),$$

where i, j, k, ℓ label external junction primaries and a, b label multiplicity channels in the relevant fusion spaces. The s-channel decomposition is

$$\mathcal{G}_{ijkl}^{ab}(\chi) = \sum_{\widehat{\mathcal{O}},\alpha,\beta} \lambda_{ij\widehat{\mathcal{O}}}^{a\alpha} \lambda_{k\ell\widehat{\mathcal{O}}}^{b\beta} C_{\alpha\beta} G_{\widehat{\Delta},\widehat{s}}(\chi),$$

where $C_{\alpha\beta}$ is the two-point metric on the exchanged multiplicity space. Crossing takes the schematic form

$$\mathcal{G}_{ijkl}^{ab}(\chi) = \sum_{c,d} \mathcal{P}_{ijkl}{}^{ab}{}_{cd} \mathcal{G}_{ikj\ell}^{cd}(1-\chi).$$

The recoupling tensor $\mathcal{P}$ is built from associators, braiding phases, and possible anomaly cocycles. Positivity in a semidefinite bootstrap does not apply directly to every component. One must first choose a reflection-positive basis of channels and then impose positive semidefiniteness on the corresponding OPE coefficient matrices.

A practical numerical program would proceed as follows.

1. Choose a finite set of external operators and sector labels.
2. Determine the allowed intermediate sectors from the refraction selection rule.
3. Compute or assume recoupling matrices $\mathcal{P}$ satisfying pentagon and reflection constraints.
4. Build defect conformal blocks appropriate to the preserved two-dimensional conformal symmetry.
5. Apply linear functionals to the crossing equations and search for positive spectra above a trial gap.
6. Repeat over trial anomaly classes and junction central charges.

The toy residual used in this paper implements only steps one, two, and a scalar version of step four. It is useful because it exposes how a putative gap and OPE weight influence crossing violation. It is not sufficient for rigorous exclusion. A future implementation should use semidefinite programming, include spinful exchanged operators, and include mixed correlators involving displacement operators and endpoint operators of refracted lines.

There is one qualitative expectation that follows already from the charge selection rule. If the monodromy image $(\mathcal{M}_{k,g} - I)\Gamma_{\text{em}}$ is large, then the set of endpoint sectors is large. A sparse low-lying spectrum is harder to reconcile with crossing because several charged channels must be represented. Conversely, when the monodromy vanishes in a finite quotient, many channels collapse and the bootstrap problem approaches that of an ordinary defect CFT.

N Numerical Convergence and Figure QA

The numerical artifacts in the package are designed to be reproducible and inspectable. The monodromy scan is exact integer arithmetic. The bootstrap residual scan is a floating-point calculation, and its stability was checked by increasing the number of cross-ratio sample points and verifying that the qualitative small-residual region remains in the same part of the $(\widehat{\Delta}_{\min}, a)$ plane.

The Matplotlib figures follow three rules. First, every figure must encode a physical or mathematical object used in the paper: a monodromy matrix, a charge lattice, a coupling trajectory, an anomaly descent, a mode profile, or a bootstrap residual. Second, schematic figures include at least one quantitative or algebraic inset whenever possible. Third, vector outputs are saved as both PDF and SVG so that journal production can choose the preferred backend.

The revised source also includes a PDF contact-sheet renderer. This is not part of the theoretical argument, but it is part of the reproducibility workflow. It catches common manuscript problems: full-page floats, clipped formulas, landscape pages that alter geometry, and oversized tables. The final manuscript was checked with this renderer after figure regeneration and LaTeX recompilation.

O Observable Dictionary

This appendix gives a practical dictionary for the observables introduced in the main text. The goal is to make clear what one would compute in a lattice regularization, a continuum path integral, a topological model, or a defect bootstrap analysis.

O.1 Refraction coefficients

The categorical refraction coefficient

$$\mathfrak{R}_\gamma{}^{\gamma'}$$

is not generally a complex amplitude. In a fully topological junction it is best understood as a vector space

$$\mathfrak{R}_\gamma{}^{\gamma'} = V_\gamma^{\gamma'}.$$

Its dimension counts the number of independent junction states that permit the incoming line L_γ to emerge as $L_{\gamma'}$. In a conformal junction, the same symbol denotes a graded space:

$$V_\gamma^{\gamma'}(q,\bar{q}) = \sum_{\widehat{\mathcal{O}}\in(\gamma,\gamma')} q^{h_{\widehat{\mathcal{O}}}-c_L/24}\bar{q}^{\bar{h}_{\widehat{\mathcal{O}}}-c_R/24}.$$

The ungraded topological coefficient is recovered by setting $q, \bar{q}$ to values appropriate for a protected index, when such an index exists. In a numerical simulation one can probe $V_\gamma^{\gamma'}$ by inserting a line ending on a small circle around the junction and measuring which outgoing line sectors have nonzero correlation functions.

The support of $\mathfrak{R}_\gamma{}^{\gamma'}$ is topological:

$$\gamma' - \rho(\gamma) \in \Lambda_\Sigma.$$

The dimensions and conformal weights inside that support are dynamical. This distinction is important. The monodromy theorem determines which sectors must be allowed or forbidden, but it does not determine how many low-energy operators appear in each allowed sector. Those multiplicities depend on the junction fixed point.

O.2 Junction entropy

For a conformal junction, the universal junction entropy may be defined by a defect partition function on a sphere or by an entanglement construction. Schematically,

$$\log g_\Sigma = \log Z[S^4;\Sigma_2] - \log Z[S^4]_{\text{bulk}} - \log Z[W_\theta] - \log Z[W_g],$$

where local power divergences and wall contributions are subtracted. In practice, the precise subtraction scheme matters. A topological sector contributes a finite degeneracy, while propagating junction modes contribute scale-dependent terms that become universal only at a fixed point.

The entropy is expected to be sensitive to categorical refraction because a junction with more allowed outgoing sectors has more endpoint states. However, $\log g_\Sigma$ is not simply the logarithm of the number of sectors. Braiding phases, anomaly constraints, and chiral central charge can change the partition function without changing the raw support of $\mathfrak{R}$.

O.3 Displacement and current data

The displacement operator measures the failure of transverse momentum conservation:

$$\partial_\mu T^{\mu i} = D^i\, \delta^{(2)}(x_\perp) + \cdots .$$

For two intersecting walls, i labels the two transverse directions, but the wall geometry can make the displacement two-point function anisotropic:

$$\langle D^i(y) D^j(0)\rangle = \frac{C_D^{ij}}{|y|^6}.$$

The matrix C_D^{ij} is a conformal datum of the junction. If the intersection angle or wall tensions are varied, C_D^{ij} changes continuously, while the monodromy class remains fixed. This makes C_D a useful diagnostic for distinguishing junction CFTs with the same topological charge data.

Similarly, conserved junction currents have two-point coefficients

$$\langle J^a(y) J^b(0)\rangle = \frac{C_J^{ab}}{|y|^2}.$$

The allowed current algebra is constrained by anomaly inflow. A chiral anomaly fixes the antisymmetric part of the current algebra level, while the symmetric positive part is dynamical and enters bootstrap positivity.

O.4 Scalar refraction index

The scalar quantity

$$n_{\mathrm{cat}}(\gamma) = \frac{1}{d_\gamma} \sum_{\gamma'} d_{\gamma'} \dim V_\gamma^{\gamma'}$$

is useful only after choosing weights d_γ. In a finite TQFT, d_γ can be the quantum dimension of the line sector. In an abelian theory all simple line quantum dimensions are one, so n_{cat} reduces to the total multiplicity of outgoing sectors. In a conformal junction, one may define a scale-dependent version by replacing $\dim V$ with a truncated character below a dimension cutoff:

$$n_{\mathrm{cat}}(\gamma; \Delta_*) = \sum_{\gamma'} \#\{\widehat{\mathcal{O}} \in V_\gamma^{\gamma'} : \widehat{\Delta} \le \Delta_*\}.$$

This object is not an optical refractive index. It is a compact summary of sector proliferation. It is invariant only under equivalences of the chosen line category and only after specifying the cutoff or index used to count states.

O.5 Monodromy invariant

The most robust observable is the conjugacy class of $\mathcal{M}_{k,g}$ acting on the exact charge quotient. For the integral lattice,

$$\mathrm{Tr}\mathcal{M}_{k,g} = 2 + k^2 c^2$$

classifies the nontrivial commutators as hyperbolic. In a finite quotient, the invariant is the conjugacy class of $\mathcal{M}_{k,g}$ in $\mathrm{SL}(2, \mathbb{Z}_N)$ or in the automorphism group of the surviving line category. This invariant can be measured by transporting a probe line around the junction and reading off its final charge. It is insensitive to local junction RG flows unless the flow changes which line operators remain genuine.

Together these quantities separate the problem into layers. The monodromy class is topological. The support of $\mathfrak{R}$ is a selection rule. The dimensions of $V_{\gamma}^{\gamma'}$ and the spectrum inside those spaces are dynamical. The coefficients $C_D, C_J, c_L - c_R$ are conformal and anomalous data. A complete classification of axion-duality junctions must specify all of these layers, not just the charge-lattice commutator.

P Reproducibility

The repository accompanying this paper contains:

- `tex/main.tex`: the LaTeX manuscript;
- `tex/refs.bib`: bibliography;
- `scripts/generate_figures.py`: symbolic calculations, numerical scans, and all figures;
- `figures/*.pdf` and `figures/*.svg`: vector figure outputs;
- `data/symbolic_monodromy.txt`: symbolic monodromy formula;
- `data/monodromy_scan.csv`: small $\mathrm{SL}(2,\mathbb{Z})$ scan;
- `data/bootstrap_residual.csv`: finite truncation residual grid;
- `data/figure_manifest.json`: figure output manifest.

To reproduce the figures, run

```
python scripts/generate_figures.py
```

from the project root. The script uses NumPy, SciPy, SymPy, and Matplotlib. No artificial-intelligence image generation or stock artwork is used.

References

[1] E. Witten, "Dyons of charge e theta over 2 pi," Phys. Lett. B **86** (1979) 283, doi:10.1016/0370-2693(79)90838-4.

[2] F. Wilczek, "Two applications of axion electrodynamics," Phys. Rev. Lett. **58** (1987) 1799, doi:10.1103/PhysRevLett.58.1799.

[3] C. G. Callan and J. A. Harvey, "Anomalies and fermion zero modes on strings and domain walls," Nucl. Phys. B **250** (1985) 427, doi:10.1016/0550-3213(85)90489-4.

[4] D. Gaiotto, A. Kapustin, N. Seiberg, and B. Willett, "Generalized global symmetries," JHEP **02** (2015) 172, arXiv:1412.5148.

[5] E. Witten, "SL(2,Z) action on three-dimensional conformal field theories with abelian symmetry," arXiv:hep-th/0307041.

[6] D. Gaiotto and E. Witten, "S-duality of boundary conditions in N=4 super Yang-Mills theory," Adv. Theor. Math. Phys. **13** (2009) 721, arXiv:0807.3720.

[7] C.-T. Hsieh, Y. Tachikawa, and K. Yonekura, "Anomaly of the electromagnetic duality of Maxwell theory," Phys. Rev. Lett. **123** (2019) 161601, arXiv:1905.08943.

[8] Y. Choi, C. Cordova, P.-S. Hsin, H. T. Lam, and S.-H. Shao, "Non-invertible duality defects in 3+1 dimensions," Phys. Rev. D **105** (2022) 125016, arXiv:2111.01139.

[9] J. Kaidi, K. Ohmori, and Y. Zheng, "Kramers-Wannier-like duality defects in (3+1)d gauge theories," Phys. Rev. Lett. **128** (2022) 111601, arXiv:2111.01141.

[10] K. Roumpedakis, S. Seifnashri, and S.-H. Shao, "Higher gauging and non-invertible condensation defects," Commun. Math. Phys. **401** (2023) 3043, arXiv:2204.02407.

[11] L. Bhardwaj, L. E. Bottini, S. Schafer-Nameki, and A. Tiwari, "Non-invertible higher-categorical symmetries," SciPost Phys. **14** (2023) 007, arXiv:2204.06564.

[12] J. Kaidi, K. Ohmori, and Y. Zheng, "Symmetry TFTs for non-invertible defects," arXiv:2209.11062.

[13] R. Yokokura, "Non-invertible symmetries in axion electrodynamics," arXiv:2212.05001.

[14] Y. Choi, H. T. Lam, and S.-H. Shao, "Non-invertible Gauss law and axions," JHEP **09** (2023) 067, arXiv:2212.04499.

[15] L. Bhardwaj and S. Schafer-Nameki, "Generalized charges, part II: non-invertible symmetries and the symmetry TFT," SciPost Phys. **19** (2025) 098, arXiv:2305.17159.

[16] N. Kan, K. Kawabata, and H. Wada, "Symmetry fractionalization and duality defects in Maxwell theory," JHEP **10** (2024) 238, arXiv:2404.14481.

[17] S. Meynet, D. Migliorati, R. Savelli, and M. Tortora, "Duality-symmetry enhancement in Maxwell theory," SciPost Phys. **19** (2025) 089, arXiv:2504.20141.

[18] F. Apruzzi and L. Martucci, "Gaillard-Zumino non-invertible symmetries," JHEP **06** (2026) 233, arXiv:2510.18997.

[19] M. Billo, V. Goncalves, E. Lauria, and M. Meineri, "Defects in conformal field theory," JHEP **04** (2016) 091, arXiv:1601.02883.

[20] P. Liendo, L. Rastelli, and B. C. van Rees, "The bootstrap program for boundary CFT_d," JHEP **07** (2013) 113, arXiv:1210.4258.

[21] F. Gliozzi, P. Liendo, M. Meineri, and A. Rago, "Boundary and interface CFTs from the conformal bootstrap," JHEP **05** (2015) 036, arXiv:1502.07217.

[22] R. A. Lanzetta, S. Liu, and M. A. Metlitski, "The beginning of the endpoint bootstrap for conformal line defects," arXiv:2508.14964.

[23] X.-L. Qi, T. L. Hughes, and S.-C. Zhang, "Topological field theory of time-reversal invariant insulators," Phys. Rev. B **78** (2008) 195424, arXiv:0802.3537.